

Global QCD fit from $Q^2 = 0$ to $Q^2 = 30000 \text{ GeV}^2$ with Regge-compatible initial condition

G. Soyez

December 25, 2018

Abstract

In this paper I show that it is possible to use Regge theory to constrain the initial parton distribution functions of a global DGLAP fit. In this approach, both quarks and gluons have the same high-energy behaviour which may also be used to describe soft interactions. More precisely, I show that, if we parametrise the parton distributions with a triple-pole pomeron, *i.e.* like $\log^2(1/x)$ at small x , at $Q^2 = Q_0^2$ and evolve these distribution with the DGLAP equation, we can reproduce F_2^p , F_2^d , F_2^n/F_2^p , $F_2^{\nu N}$ and $xF_3^{\nu N}$ for $W^2 \geq 12.5 \text{ GeV}^2$. In this case, we obtain a new leading-order global QCD fit with a Regge-compatible initial condition.

I shall also show that it is possible to use Regge theory to extend the parton distribution functions to small Q^2 . This leads to a description of the structure functions over the whole Q^2 range based on Regge theory at low Q^2 and on QCD at large Q^2 .

Finally, I shall argue that, at large Q^2 , the parton distribution functions obtained from DGLAP evolution and containing an essential singularity at $j = 1$ can be approximated by a triple-pole pomeron behaviour.

1 Introduction

About thirty years ago, Dokshitzer, Gribov, Lipatov, Altarelli and Parisi have shown [1] that quantum chromodynamics predicts a breakdown of Bjorken scaling in Deep Inelastic Scattering (DIS). Once the parton distribution functions are fixed at one initial scale $Q^2 = Q_0^2$, the DGLAP equation gives their evolution to larger values of Q^2 . Although the initial equation has only included QCD contributions at leading order (LO) in α_s , the next-to-leading order (NLO) corrections are now known as well as the NNLO corrections. There exists a rather large number of global fits (e.g. [2, 3, 4, 5, 6]) using the DGLAP equation to reproduce the DIS data. The basic idea is to fix the initial parton distributions, not predicted by perturbative QCD (pQCD), and to evolve it in order to reproduce the experimental measurements as well as possible. The success of this type of analysis is often considered as one of the most important prediction of pQCD. However, it appears that this approach presents some problems. Firstly, even if the strong rise of F_2 observed by HERA at

small x is well reproduced by the DGLAP evolution, this may seem surprising since the evolution generates an unphysical essential singularity which should be replaced by the BFKL small- x behaviour [7] which is not observed in the data and is unstable against NLO corrections [8]. In addition, since the initial parton distributions are not predicted by pQCD, we have to parametrise them. This introduces a large number of free parameters in the models.

In this paper, we shall study the possibility to use Regge theory [9, 10, 11] to constrain the initial parton distributions used in QCD global fits. To motivate this approach, one can, for example, consider the MRST2002 initial conditions: at small x , we have

$$\begin{aligned} xq(x, Q_0^2) &= Ax^{-0.12}, \\ xg(x, Q_0^2) &= Bx^{-0.27} + Cx^{0.00}. \end{aligned}$$

These singularities in x do not correspond to any singularity present in hadronic cross sections [12, 13, 14, 15] and, conversely, cross-section singularities are not present in parton distributions. There should therefore exist a mechanism explaining how the residues of these singularities in partonic distributions vanish when Q^2 goes to zero, and how the residues of the singularities observed in the total cross sections vanish for nonzero Q^2 . Such a mechanism is unknown and seems forbidden in Regge theory, hence a description of both total cross sections and partonic distributions with the same singularity structure seems necessary.

In a previous work [16], we have shown that, if one considers only the small- x and large- Q^2 domain, one can use a triple-pole pomeron (squared logarithm of x) to reproduce the low- Q^2 data and evolve it using the DGLAP equation to obtain the high- Q^2 measurements. More precisely, we have used parametrisations of the form

$$A \log^2(1/x) + B \log(1/x) + C + D \left(\frac{1}{x} \right)^{-\eta}$$

for initial quark and gluon distributions. Since this Regge-constrained parametrisation does not extend to $x = 1$, we have used the GRV parton distributions at large x ($x \geq x_{\text{Regge}} \approx 0.15$). As a consequence, only two quark distributions were needed (a flavour singlet coupled to gluons and a flavour non-singlet) and only the proton structure function was fitted.

In this paper, we shall extend the triple-pole parametrisation up to $x = 1$ in order to obtain a global QCD fit compatible with Regge theory at small Q^2 . At first sight, if we want to replace the GRV parton distributions at large x , we can, for example, introduce powers of $(1 - x)$. However, if we do so, we must not only concentrate on the Regge domain but also on the large- x experimental measurements, including other experiments like γ^*d scattering and the neutrino data. We shall fit all structure functions over the whole x range at all scales greater than Q_0^2 . This will allow us to extract the parton distribution functions, which will be parametrised in such a way that they agree with Regge theory at small values of x .

In this study, we shall also consider the extension of the Regge initial parametrisation to low- Q^2 values. Using standard techniques, we shall show that it is possible to continue the initial parton distributions to small Q^2 .

Finally, we shall show that, at large Q^2 , the parton distributions obtained from DGLAP evolution, containing an essential singularity, can be approximated by a squared logarithm of $1/x$ within estimated DGLAP uncertainties. This confirms the results obtained in [17] where we have shown that the residues of the triple-pole pomeron can be extracted from DGLAP evolution.

We should also point out that a similar type of approach has already been used by Donnachie and Landshoff [18], and by Csernai, Jenkovszky, Kontros, Lengyel Magas and Paccanoni [19]. However, our approach is different from their work in a number of points. Firstly, we keep the full DGLAP evolution equation, without taking only the residue at the leading singularity as done by Donnachie and Landshoff. In addition, the work by Csernai *et al.* only reproduces F_2^p which means that they only need two quark distributions: a flavour singlet and a flavour non-singlet, only the flavour-singlet distribution being parametrised using Regge theory. Their present work extends these ideas and those of [16, 17] to provide a standard set¹ of structure functions, which reproduces the data for all values of x and Q^2 .

2 Fitted and evolved quantities

If we want to extend the parametrisation introduced in [16] up to $x = 1$, we cannot only restrict ourselves to F_2^p . In order to have a good determination of the valence quarks and of the sea asymmetry, we also need to include other structure functions, measured in the large- x region. In this global fit, we thus include the following quantities:

- The proton structure function F_2^p [21, 22, 23, 24, 25, 26, 27, 28, 29, 30, 31, 32, 33, 34, 35, 36, 37, 38, 39]: this is by far the most important type of experimental data. Moreover, it is nearly the only one to contribute to the fit in the small- x or in the high- Q^2 region.
- The deuteron structure function F_2^d [37, 38, 39, 40]: as we shall see, these data allow the determination of the sea asymmetry. Many points are available in the large- and middle- x regions, where the sea asymmetry is expected to be large.
- The neutrino structure functions $F_2^{\nu N}$ and $F_3^{\nu N}$ [42, 43, 44]: these data, in which most of the points are at large values of x , are important to fix the strange quark and the valence quark distributions. Note that the data considered here are averaged over neutrinos and anti-neutrinos.
- The F_2^n/F_2^p measurements [41]: these data constrain the valence quark distributions and the sea asymmetry.

¹A C code for this standard set is available at <http://lepton.theo.phys.ulg.ac.be/~soyez>.

Once we know which experiments are fitted, we must find which quantities need to be evolved. Since the Q^2 range under consideration in global fits extends up to 30000 GeV², we need to consider 5 quark flavours: u , d , s , c and b . In order to use DGLAP evolution, it is easier to perform linear combinations of the quark distributions. In our case, we shall use 6 flavour-non-singlet distributions

$$\begin{aligned}
xu_V &= x(u - \bar{u}), \\
xd_V &= x(d - \bar{d}), \\
T_3 &= x(u^+ - d^+), \\
T_8 &= x(u^+ + d^+ - 2s^+), \\
T_{15} &= x(u^+ + d^+ + s^+ - 3c^+), \\
T_{24} &= x(u^+ + d^+ + s^+ + c^+ - 4b^+),
\end{aligned} \tag{1}$$

where $q^+ = q + \bar{q}$. Note that since the proton does not contain constituent strange, charm or bottom valence quarks, we have $s = \bar{s}$, $c = \bar{c}$ and $b = \bar{b}$. At leading order, the Q^2 evolution of each of these distributions is given by the DGLAP equation with the splitting $xP_{qq}(x)$. In addition to the non-singlet distributions, we have the singlet quark distribution

$$\Sigma = x(u^+ + d^+ + s^+ + c^+ + b^+)$$

which evolves coupled to the gluon distribution $G = xg$, with the full splitting matrix

$$\begin{pmatrix} xP_{qq}(x) & 2n_f xP_{qg}(x) \\ xP_{gq}(x) & xP_{gg}(x) \end{pmatrix}.$$

We shall assume that for $Q^2 \leq 4m_q^2$, the quark q does not enter into the evolution equations.

If we invert the relations (1) and express the quark densities q^+ in terms of the evolved quantities, we obtain

$$\begin{aligned}
xu^+ &= \frac{1}{60}(12\Sigma + 3T_{24} + 5T_{15} + 10T_8 + 30T_3), \\
xd^+ &= \frac{1}{60}(12\Sigma + 3T_{24} + 5T_{15} + 10T_8 - 30T_3), \\
xs^+ &= \frac{1}{60}(12\Sigma + 3T_{24} + 5T_{15} - 20T_8), \\
xc^+ &= \frac{1}{20}(4\Sigma + T_{24} - 5T_{15}), \\
xb^+ &= \frac{1}{5}(\Sigma - T_{24}).
\end{aligned}$$

Now, we can of course write the structure functions considered here in terms of the parton distributions or in terms of the flavour-singlet and flavour-non-singlet

distributions². If, for the sake of clarity, we include other quantities like the neutron structure function, this gives

$$\begin{aligned}
F_2^p &= \frac{4x}{9}(u^+ + c^+) + \frac{x}{9}(d^+ + s^+ + b^+) \\
&= \frac{1}{90}(22\Sigma + 3T_{24} - 5T_{15} + 5T_8 + 15T_3), \\
F_2^n &= \frac{4x}{9}(d^+ + c^+) + \frac{x}{9}(u^+ + s^+ + b^+) \\
&= \frac{1}{90}(22\Sigma + 3T_{24} - 5T_{15} + 5T_8 - 15T_3), \\
F_2^d &= \frac{F_2^p + F_2^n}{2} \\
&= \frac{5x}{18}(u^+ + d^+) + \frac{4x}{9}c^+ + \frac{x}{9}(s^+ + b^+) \\
&= \frac{1}{90}(22\Sigma + 3T_{24} - 5T_{15} + 5T_8),
\end{aligned}$$

and for the neutrino structure functions

$$\begin{aligned}
F_2^{\nu p} &= 2x(d + s + b + \bar{u} + \bar{c}), \\
F_2^{\nu n} &= 2x(u + s + b + \bar{d} + \bar{c}), \\
F_2^{\bar{\nu} p} &= 2x(u + c + \bar{d} + \bar{s} + \bar{b}), \\
F_2^{\bar{\nu} n} &= 2x(d + c + \bar{u} + \bar{s} + \bar{b}), \\
xF_3^{\nu p} &= 2x(d + s + b - \bar{u} - \bar{c}), \\
xF_3^{\nu n} &= 2x(u + s + b - \bar{d} - \bar{c}), \\
xF_3^{\bar{\nu} p} &= 2x(u + c - \bar{d} - \bar{s} - \bar{b}), \\
xF_3^{\bar{\nu} n} &= 2x(d + c - \bar{u} - \bar{s} - \bar{b}),
\end{aligned}$$

If we average over proton and neutron targets, we obtain the neutrino-nucleon structure functions³

$$\begin{aligned}
F_2^{\nu N} = F_2^{\bar{\nu} N} &= x(u^+ + d^+ + s^+ + c^+ + b^+), \\
xF_3^{\nu N} &= x(u_V + d_V + s^+ - c^+ + b^+), \\
xF_3^{\bar{\nu} N} &= x(u_V + d_V - s^+ + c^+ - b^+).
\end{aligned}$$

²At leading order, the quark coefficient functions are proportional to $\delta(1-x)$ and the gluon coefficient function vanishes.

³Neutrino experiments are often performed with heavy nuclei which means that the averaged structure function is measured.

We may finally average over neutrinos and anti-neutrinos, which leads to

$$\begin{aligned} F_2^{(\bar{\nu})N} &= x(u^+ + d^+ + s^+ + c^+), \\ &= \Sigma, \\ xF_3^{(\bar{\nu})N} &= x(u_V + d_V). \end{aligned}$$

3 Initial parametrisation

If we want to perform a DGLAP evolution, we need to fix the parton distribution functions at an initial scale Q_0^2 . Following the same ideas as in [16], we shall parametrise each quark distribution as the sum of a triple-pole pomeron term and an a_2/f -reggeon term. In addition, each distribution will be multiplied by a power of $(1-x)$, to ensure that the parametrisation extended to $x = 1$ goes to 0 when $x \rightarrow 1$. This leads to the following parametrisation

$$xq(x, Q_0^2) = [A_q \log^2(1/x) + B_q \log(1/x) + C_q + D_q x^\eta] (1-x)^{b_q},$$

with⁴ $q = u_V, d_V, u_s, d_s, s_s, c_s$ and g . Fortunately, we can restrict many of the 35 parameters introduced here:

- First of all, the charm (bottom) distribution will be set to zero for $Q^2 \leq 4m_c^2$ ($Q^2 \leq 4m_b^2$). We shall therefore take $Q_0^2 \leq 4m_c^2$ so that we can set $c(x, Q_0^2) = 0$ and $b(x, Q_0^2) = 0$. In other words, we have $T_{15}(x, Q^2) = \Sigma(x, Q^2)$ for $Q^2 \leq 4m_c^2$ and $T_{24}(x, Q^2) = \Sigma(x, Q^2)$ for $Q^2 \leq 4m_b^2$.
- The pomeron does not distinguish between quarks and anti-quarks. This means that the valence distributions u_V and d_V do not contain a pomeron term.
- The pomeron, having vacuum quantum numbers, is insensitive to quark flavour. Thus, the only parameter through which the quark flavour may influence the pomeron is its mass. In other words, the couplings A_q, B_q and C_q are functions of Q^2 and m_q^2 only. Consequently, the pomeron contributions to the u_s and d_s densities are the same. Assuming that the strange mass is very small compared to the virtualities Q^2 under consideration, we shall also take the same pomeron contribution⁵ in s_s .

$$\begin{aligned} A_u &= A_d = A_s = A, \\ B_u &= B_d = B_s = B, \\ C_u &= C_d = C_s = C. \end{aligned}$$

⁴The sea distribution q_s is simply $\frac{1}{2}q^+$.

⁵If we insert an overall factor in s_s , the fit naturally sets it to 1.

- We shall assume that the reggeon, being mainly constituted of quarks, does not contribute to the gluon distribution. The parameter D_g will thus⁶ be set to 0.
- We know from [20] that, at large x , the following behaviour is stable with respect to DGLAP evolution

$$\begin{aligned}\Sigma &\sim (1-x)^b, \\ G &\sim \frac{(1-x)^{b+1}}{\log\left(\frac{1}{1-x}\right)}.\end{aligned}$$

The denominator $\log(1-x)$ in the gluon distribution does not have a good behaviour at small x so we have not included it⁷. Nevertheless, we shall impose

$$\begin{aligned}b_u &= b_d = b_s = b, \\ b_g &= b + 1.\end{aligned}$$

- If we look at the large- x data, we can see that if we only use $Dx^\eta(1-x)^b$ for the valence quarks, the resulting distribution is too wide, or has a peak at too small a value of x . In order to solve that problem, we have multiplied the valence-quark distributions by a factor $(1 + \gamma_q x)$.
- Finally, we still need to impose sumrules. Quark-number conservation can be used to fix the valence-quark normalisation factors. If we write

$$A_{uV} = \frac{2}{N_u} \quad \text{and} \quad A_{dV} = \frac{1}{N_d},$$

we find

$$N_q = \frac{\Gamma(b_q + 1)\Gamma(\eta)}{\Gamma(\eta + b_q + 1)} \left(1 + \frac{\gamma_q \eta}{\eta + b_q + 1}\right). \quad (2)$$

The momentum sumrule is used to fix the constant term C_g in the gluon distribution. Although all the functions involved are analytically integrable, the resulting expression for C_g is quite complicated and we give it in appendix.

⁶If we do not impose $D_g = 0$, the parameter stays small in the fit.

⁷One solution is to multiply the gluon distribution by an overall factor x . This makes no change at large x and ensures a good behaviour at small x because, when $x \rightarrow 0$,

$$\frac{x}{\log\left(\frac{1}{1-x}\right)} \rightarrow 1.$$

Numerically, including this factor in the gluon distribution only makes a small correction.

Taking all these considerations into account, we obtain the following parametrisation for the initial distributions

$$\begin{aligned}
xu_V &= \frac{2}{N_u^*} x^\eta (1 + \gamma_u x) (1 - x)^{b_u}, \\
xd_V &= \frac{1}{N_d^*} x^\eta (1 + \gamma_d x) (1 - x)^{b_d}, \\
xu_s &= [A \log^2(1/x) + B \log(1/x) + C + D_u x^\eta] (1 - x)^b, \\
xd_s &= [A \log^2(1/x) + B \log(1/x) + C + D_d x^\eta] (1 - x)^b, \\
xs_s &= [A \log^2(1/x) + B \log(1/x) + C + D_s x^\eta] (1 - x)^b, \\
xc_s &= 0, \\
xb_s &= 0, \\
xg &= [A_g \log^2(1/x) + B_g \log(1/x) + C_g^*] (1 - x)^{b+1},
\end{aligned} \tag{3}$$

where the parameters marked with an asterisk are constrained by sumrules.

4 Fitted experiments

As said previously, we have fitted F_2^p , F_2^d , $F_2^{\nu N}$, $xF_3^{\nu N}$ and F_2^n/F_2^p . We shall now detail which experiments are included in the fit for all these quantities.

For the proton structure function, we have fitted the experiments from⁸ H1 [21, 22, 23, 24, 25, 26, 27], ZEUS [28, 29, 30, 31, 32, 33, 34, 35], BCDMS [36], E665 [37], NMC [38] and SLAC [39]. For the deuteron structure function measurements, we have included data from BCDMS [40] E665 [37] and NMC [38]. We have also taken into account the measurements of F_2^n/F_2^p from NMC [41]. Finally, the neutrino data used here come from CCFR [42, 43, 44].

Among all these experimental papers, some give, besides the statistical and the systematic errors, an additional normalisation uncertainty. For each of these subsets of the data, we have allowed an overall normalisation factor. Let R_i be the normalisation uncertainty for the subset i , and ρ_i the effective normalisation factor. We may easily minimise the χ^2 with respect to this parameter by requiring

$$\frac{\partial \chi^2}{\partial \rho_i} = \frac{\partial}{\partial \rho_i} \sum_j \frac{(\rho_i d_j - t_j)^2}{\varepsilon_j^2} = 0,$$

where j runs over the data in the subset i , d_j , ε_j and t_j are respectively the j th data, its uncertainty and the associated theoretical prediction. We easily find

$$\rho_i = \frac{\sum_j \frac{d_j t_j}{\varepsilon_j^2}}{\sum_j \frac{d_j^2}{\varepsilon_j^2}}.$$

⁸The dataset is coming from the DURHAM database (<http://durpdg.dur.ac.uk>) to which we have added the 2000 and 2001 data from HERA [26, 27, 35] as well as the reanalysed CCFR 2001 data [44].

Parameter	Value	Error
A	0.00876	0.00043
B	0.0197	0.0035
C	0.000	0.017
A_g	0.258	0.032
B_g	-0.62	0.25
D_u	0.378	0.030
D_d	0.480	0.030
D_s	0.000	0.013
η	0.392	0.019
γ_u	7.46	0.91
γ_d	9.1	1.6
b_u	3.625	0.016
b_d	5.261	0.086
b	6.67	0.27
N_u	2.015	-
N_d	1.723	-
C_g	3.158	-

Table 1: Values of the fitted parameters in the parton distributions. The last three parameters are not fitted but are obtained from sum-rules.

Finally, we shall require that ρ_i does not lead to a normalisation bigger than the uncertainty R_i . This means that we shall constrain ρ_i to verify

$$1 - R_i \leq \rho_i \leq 1 + R_i.$$

Before going to the result, one must point out that we have used here the latest CCFR data⁹ from 2001 [44]. These data from U.K. Yang's thesis are used by adding the errors in quadrature and, in order to solve a discrepancy with the other data, we have also allowed an overall normalisation factor of at most 3%.

⁹They consist into a reanalysis of the 1997 data.

Experiment information					This fit		CTEQ6 LO		CTEQ6 NLO	
Quant.	Colab.	Reference	Nb Pts	ρ_i (%)	χ^2	χ^2/nop	norm.	\neg norm.	norm.	\neg norm.
F_2^p	BCDMS	PLB223(1989)485	167	-	154.607	0.926	5.303	5.303	2.652	2.652
	E665	PRD54(1996)3006	30	1.80	40.368	1.346	1.177	1.233	1.251	1.383
	H1	EPJC19(2001)269	126	-1.50	129.673	1.029	1.516	1.626	1.077	1.122
		EPJC21(2001)33	86	-	75.774	0.881	0.942	0.942	1.008	1.008
		EPJC13(2000)609	130	-1.50	117.682	0.905	1.612	1.962	0.882	1.032
		NPB470(1996)3	156	-	104.206	0.668	0.835	0.835	0.658	0.658
		NPB439(1995)471	90	-4.50	49.499	0.550	0.597	0.901	0.574	0.737
		NPB407(1993)515	21	-8.00	6.233	0.297	0.289	0.466	0.287	0.401
	NMC	NPB483(1997)3	79	2.10	101.927	1.290	1.728	1.260	1.138	1.186
	SLAC	PLB282(1992)475	52	-	97.861	1.882	2.123	2.123	1.355	1.355
	ZEUS	EPJC21(2001)443	214	-	207.294	0.969	2.454	2.454	0.875	0.875
		EPJC7(1999)609	12	-	11.297	0.941	0.744	0.744	1.259	1.259
		ZPC72(1996)399	172	-	238.882	1.389	1.299	1.299	1.429	1.429
		ZPC65(1995)379	56	2.00	27.477	0.491	0.495	0.415	0.453	0.470
		ZPC69(1995)607	9	-1.54	11.493	1.277	1.201	1.270	1.309	1.289
		PLB316(1993)412	17	6.94	6.048	0.356	0.370	0.372	0.344	0.474
	Total		1417		1380.321	0.974	1.864	1.900	1.150	1.187
F_2^d	BCDMS	PLB237(1989)592	154	-	127.941	0.831	1.546	1.546	0.903	0.903
	E665	PRD54(1996)3006	30	-	33.563	1.119	0.913	0.913	1.132	1.132
	NMC	NPB483(1997)3	79	1.00	90.330	1.143	1.438	1.131	0.969	1.071
	SLAC	SLAC-357(1990)	50	-	98.376	1.968	2.515	2.515	1.278	1.278
	Total		313		350.210	1.119	1.613	1.536	1.002	1.027
$F_2^{\nu N}$	CCFR	UK. Yang's thesis	65	3.00	165.512	2.546	3.118	4.570	3.523	6.135
$xF_3^{\nu N}$	CCFR	PRL79(1997)1213	76	-	42.066	0.554	0.658	0.658	1.252	1.252
F_2^n/F_2^p	NMC	NPB371(1995)3	91	-	116.720	1.283	1.315	1.315	1.285	1.285
Total			1962		2054.830	1.047	1.794	1.855	1.215	1.333

Table 2: Fit results detailed experiment by experiment. For comparison we have added the predictions for CTEQ6 at leading and next-to-leading order (the NLO predictions are taken in the DIS scheme). In the comparison with CTEQ, the results are given with and without taking into account our normalisation factors.

5 Results of the DGLAP global fit

We have adjusted the 14 parameters $A, B, C, A_g, B_g, D_u, D_d, D_s, b, b_u, b_d, \gamma_u, \gamma_d$ and η to the experimental data in the region

$$\begin{aligned} Q^2 &\geq 4m_c^2 = 6.76 \text{ GeV}^2, \\ W^2 &\geq 12.5 \text{ GeV}^2. \end{aligned}$$

The second boundary is used to cut the region where higher-twists effects are expected to be large and we have adopted the same limit on W^2 as MRST. The values of the fitted parameters are presented in Table 1 and the result, detailed experiment by experiment, is given in Table 2. In addition, the curves resulting from our fit are presented for each experiment in Figures 3 to 15.

We can see from the parameter table that both the large- x exponents and the reggeon intercept have acceptable values.

In order to evaluate the quality of our fit, we have also shown in Table 2 the CTEQ6 results at LO and at NLO (in the DIS scheme¹⁰), with and without taking the normalisation factors into account¹¹. We see that the CCFR 2001 neutrino data probably need to be renormalised up and are still poorly reproduced. We can also see that, apart from the SLAC data, we obtain a very good description. This means that it would be a good idea to add a renormalisation factor of a few percents to the SLAC F_2^p and F_2^d data.

The correlation matrix for the parameters is presented in Table 5.

In Figure 1, we have shown some typical distributions and their Q^2 evolution. The xu_V and xd_V valence quarks distributions both present a peak around $x \approx 0.1 - 0.2$ and are, roughly speaking, within a factor 2. The sea asymmetry $\bar{d} - \bar{u}$ can be written in the following form:

$$\begin{aligned} x(\bar{d} - \bar{u}) &= \frac{xu_V - xd_V - T_3}{2} \\ &= (D_d - D_u)x^\eta(1-x)^b. \end{aligned}$$

This distribution has a maximum for

$$x = \frac{\eta}{b + \eta} \approx \begin{cases} 0.1 & \text{for } xu_V, \\ 0.07 & \text{for } xd_V, \\ 0.056 & \text{for } x(\bar{d} - \bar{u}). \end{cases}$$

The evolution in Q^2 of these three distribution shows the same behaviour: the peak is moved to smaller values of x and tamed while its width grows. We have also shown in Figure 1 the gluon distribution which grows quickly with Q^2 .

¹⁰The DIS scheme is the renormalisation scheme where, at any order, the quark coefficient function is $\delta(1-x)$ and the gluon coefficient function vanishes.

¹¹The CTEQ6 results are obtained by using the last CTEQ parton distributions to predict structure functions without any refit. Therefore, the LO and NLO results are just given for comparison.

The parton densities at various scales are plotted in Figure 2. First of all, when $Q^2 = Q_0^2 = 4m_c^2$, we have no charm or bottom quark and both quark and gluon distributions are described by Regge theory, more precisely by a triple-pole and a reggeon contribution. At higher virtualities, charm quarks are non-vanishing and, for $Q^2 > 4m_b^2$, we also have b quarks. For $Q^2 > Q_0^2$, the parton distributions have an essential singularity at $j = 1$.

Finally, we can estimate the uncertainty on the initial distributions in the following way: for the sea quarks or for the gluon, we have ($D = 0$ for the gluon distribution)

$$xq = [A \log^2(1/x) + B \log(1/x) + C + Dx^\eta] (1-x)^b.$$

If we assume that the uncertainties on the parameters are uncorrelated, we obtain easily

$$\begin{aligned} (\delta xq)^2 &= \{ \log^4(1/x) \delta A^2 + \log^2(1/x) \delta B^2 + \delta C^2 + [\delta D^2 + \log^2(1/x) D^2 \delta \eta^2] x^{2\eta} \\ &+ [A \log^2(1/x) + B \log(1/x) + C + Dx^\eta] \log^2(1-x) \delta b^2 \} (1-x)^{2b}. \end{aligned}$$

For the valence quarks, the initial distribution has the form

$$xq_V = K x^\eta (1-x)^b (1+\gamma x)$$

with K fixed by quark number conservation, and we find that the uncertainty is

$$(\delta xq)^2 = K^2 x^{2\eta} (1-x)^{2b} \{ [\log^4(1/x) \delta \eta^2 + \log^2(1-x) \delta b^2] (1+\gamma x)^2 + x^2 \delta \gamma^2 \}.$$

The resulting uncertainties on the initial distributions are shown in Figure 16, where we have also plotted the uncertainties obtained by taking into account correlations between the parameters (see Table 5). We see that this “traditional” way of estimating errors leads to much smaller uncertainties than the joint consideration of forward and backward evolution obtained in [17].

6 Regge theory at low Q^2

6.1 Motivation

If DGLAP evolution gives the behaviour of the parton distributions at large Q^2 , we expect soft physics to be described by Regge theory. In other words, Regge theory should not only be able to describe the initial DGLAP condition but also the structure functions for $0 \leq Q^2 \leq Q_0^2$. In this section, we shall therefore try to extend the parton distribution functions at low values of Q^2 . Note that in this region, we cannot use the DGLAP equation anymore. In addition, if we want to use Regge theory, we must still restrict ourselves to the high-energy domain. Hence we keep the constraint

$$W^2 \geq 12.5 \text{ GeV}^2$$

but allow Q^2 to be in the region

$$0 \leq Q^2 \leq 6.76 \text{ GeV}^2.$$

Experiment information					This fit	
Quant.	Colab.	Reference	Nb Pts	Norm.	χ^2	χ^2/nop
F_2^p	E665	PRD54(1996)3006	61	1.80	55.265	0.906
	H1	NPB439(1995)471	3	-4.50	0.834	0.278
		NPB470(1996)3	37	-	15.518	0.419
		NPB497(1996)3	44	-3.00	35.660	0.810
		EPJC21(2001)33	47	-	61.721	1.313
	NMC	NPB483(1997)3	67	2.10	46.473	0.694
	SLAC	PLB282(1992)475	94	-	102.417	1.090
	ZEUS	ZPC69(1995)607	14	1.54	29.452	2.104
		ZPC72(1996)399	16	-	11.339	0.709
		PLB407(1997)432	34	-	10.753	0.316
		EPJC7(1999)609	32	-	34.541	1.079
		EPJC12(2000)35	70	-	86.120	1.230
		EPJ21(2001)443	28	-	48.034	1.716
	Total		547	-	538.127	0.984
F_2^d	E665	PRD54(1996)3006	61	-	76.977	1.262
	NMC	NPB483(1997)3	67	1.00	40.064	0.598
	SLAC	SLAC-357(1990)	98	-	86.511	0.883
		PRD49(1994)5641	1	0.89	0.000	0.000
	Total		227	-	203.552	0.897
$F_2^{\nu N}$	CCFR	UK. Yang's thesis	19	3.00	63.159	3.325
$xF_3^{\nu N}$	CCFR	PRL79(1997)1213	35	-	39.201	1.120
F_2^n/F_2^p	NMC	NPB371(1995)3	120	-	101.445	0.845
Total			948	-	945.485	0.997

Table 3: Result of the small- Q^2 fit detailed experiment by experiment.

Parameter	Value	Error
$a_{\mathcal{B}}$	15.05	1.80
$Q_{\mathcal{A}}^2$	6.37	2.72
$Q_{\mathcal{B}}^2$	1.885	0.522
$Q_{\mathcal{C}}^2$	10.00	8.70
$Q_{\mathcal{D}_u}^2$	0.437	1.07
$Q_{\mathcal{D}_d}^2$	5.19	3.11
Q_b^2	3.64	1.87
$Q_{b_u}^2$	5.10	2.38
$Q_{b_d}^2$	87.9	15.8
$\varepsilon_{\mathcal{A}}$	1.002	0.328
$\varepsilon_{\mathcal{B}}$	0.581	0.110
$\varepsilon_{\mathcal{C}}$	18.19	4.37
$\varepsilon_{\mathcal{D}_u}$	0.340	0.157
$\varepsilon_{\mathcal{D}_d}$	1.618	0.615
ε_b	1.916	0.453
ε_{b_u}	2.558	0.593
ε_{b_d}	10.00	6.94

Table 4: Value of the parameters with their errors for the low- Q^2 fit. The scales are given in GeV^2 .

6.2 Small- Q^2 parametrisation

If we want to use Regge theory in the small- Q^2 region, we need to parametrise the parton distribution functions. We shall use the same expressions as in (3) with an additional Q^2 dependence. However, if we want to consider the extension down to $Q^2 = 0$, we know that we should use the Regge variable $\nu = \frac{Q^2}{2x}$ instead of x . This means that we shall use the following distributions:

$$\begin{aligned}
xu_V(\nu, Q^2) &= \frac{2}{N_u^*} (2\nu)^{-\eta} \left[1 + \gamma_u(Q^2) \frac{Q^2}{2\nu} \right] \left(1 - \frac{Q^2}{2\nu} \right)^{b_u(Q^2)}, \\
xd_V(\nu, Q^2) &= \frac{1}{N_d^*} (2\nu)^{-\eta} \left[1 + \gamma_d(Q^2) \frac{Q^2}{2\nu} \right] \left(1 - \frac{Q^2}{2\nu} \right)^{b_d(Q^2)}, \\
xu_s(\nu, Q^2) &= \left\{ \mathcal{A}(Q^2) [\log(2\nu) - \mathcal{B}(Q^2)]^2 + \mathcal{C}(Q^2) + \mathcal{D}_u(Q^2) (2\nu)^{-\eta} \right\} \left(1 - \frac{Q^2}{2\nu} \right)^{b(Q^2)}, \\
xd_s(\nu, Q^2) &= \left\{ \mathcal{A}(Q^2) [\log(2\nu) - \mathcal{B}(Q^2)]^2 + \mathcal{C}(Q^2) + \mathcal{D}_d(Q^2) (2\nu)^{-\eta} \right\} \left(1 - \frac{Q^2}{2\nu} \right)^{b(Q^2)}, \\
xs_s(\nu, Q^2) &= \left\{ \mathcal{A}(Q^2) [\log(2\nu) - \mathcal{B}(Q^2)]^2 + \mathcal{C}(Q^2) + \mathcal{D}_s(Q^2) (2\nu)^{-\eta} \right\} \left(1 - \frac{Q^2}{2\nu} \right)^{b(Q^2)},
\end{aligned} \tag{4}$$

where, once again, N_u and N_d are constrained by quark number conservation. We shall require that the parameters in these distributions match the initial distribution taken for DGLAP evolution at 6.76 GeV². Using parametrisations of the form¹²

$$\begin{aligned}\phi(Q^2) &= a_\phi Q^2 \left(\frac{Q_\phi^2}{Q^2 + Q_\phi^2} \right)^{\varepsilon_\phi} & \text{for } \phi = \mathcal{A}, \mathcal{C}, \mathcal{D}_u, \mathcal{D}_d, b, b_u, b_d \\ \mathcal{B}(Q^2) &= a_{\mathcal{B}} \left(\frac{Q^2}{Q^2 + Q_{\mathcal{B}}^2} \right)^{\varepsilon_{\mathcal{B}}} + a_{\mathcal{B}}^* \\ \gamma_i(Q^2) &= \gamma_i(Q_0^2) & \text{for } i = u, d, \\ \mathcal{D}_s &= 0\end{aligned}$$

and constraining the parameters $a_{\mathcal{A}}, a_{\mathcal{B}}^*, a_{\mathcal{C}}, a_{\mathcal{D}_u}, a_{\mathcal{D}_d}, a_{\mathcal{D}_s}, a_b, a_{b_u}$ and a_{b_d} with the DGLAP initial condition at $Q^2 = Q_0^2 = 6.76 \text{ GeV}^2$, we are left with 17 parameters: $a_{\mathcal{B}}, Q_{\mathcal{A}}^2, Q_{\mathcal{B}}^2, Q_{\mathcal{C}}^2, Q_{\mathcal{D}_u}^2, Q_{\mathcal{D}_d}^2, Q_b^2, Q_{b_u}^2, Q_{b_d}^2, \varepsilon_{\mathcal{A}}, \varepsilon_{\mathcal{B}}, \varepsilon_{\mathcal{C}}, \varepsilon_{\mathcal{D}_u}, \varepsilon_{\mathcal{D}_d}, \varepsilon_b, \varepsilon_{b_u}, \varepsilon_{b_d}$. The expressions obtained once the constrained have been imposed are the following:

$$\begin{aligned}\mathcal{A}(Q^2) &= A \frac{Q^2}{Q_0^2} * \left(\frac{Q_0^2 + Q_{\mathcal{A}}^2}{Q^2 + Q_{\mathcal{A}}^2} \right)^{\varepsilon_{\mathcal{A}}} \\ \mathcal{B}(Q^2) &= a_{\mathcal{B}} \left[\left(\frac{Q^2}{Q^2 + Q_{\mathcal{B}}^2} \right)^{\varepsilon_{\mathcal{B}}} - \left(\frac{Q_0^2}{Q_0^2 + Q_{\mathcal{B}}^2} \right)^{\varepsilon_{\mathcal{B}}} \right] + \log(Q_0^2) - \frac{B}{2A} \\ \mathcal{C}(Q^2) &= \left(C - \frac{B^2}{4A} \right) \frac{Q^2}{Q_0^2} \left(\frac{Q_0^2 + Q_{\mathcal{C}}^2}{Q^2 + Q_{\mathcal{C}}^2} \right)^{\varepsilon_{\mathcal{C}}} \\ \mathcal{D}_u(Q^2) &= D_u \frac{Q^2}{Q_0^2} (Q_0^2)^\eta \left(\frac{Q_0^2 + Q_{\mathcal{D}_u}^2}{Q^2 + Q_{\mathcal{D}_u}^2} \right)^{\varepsilon_{\mathcal{D}_u}} \\ \mathcal{D}_d(Q^2) &= D_d \frac{Q^2}{Q_0^2} (Q_0^2)^\eta \left(\frac{Q_0^2 + Q_{\mathcal{D}_d}^2}{Q^2 + Q_{\mathcal{D}_d}^2} \right)^{\varepsilon_{\mathcal{D}_d}} \\ \mathcal{D}_s(Q^2) &= 0 \\ b(Q^2) &= b \frac{Q^2}{Q_0^2} * \left(\frac{Q_0^2 + Q_b^2}{Q^2 + Q_b^2} \right)^{\varepsilon_b} \\ b_u(Q^2) &= b_u \frac{Q^2}{Q_0^2} * \left(\frac{Q_0^2 + Q_{b_u}^2}{Q^2 + Q_{b_u}^2} \right)^{\varepsilon_{b_u}} \\ b_d(Q^2) &= b_d \frac{Q^2}{Q_0^2} * \left(\frac{Q_0^2 + Q_{b_d}^2}{Q^2 + Q_{b_d}^2} \right)^{\varepsilon_{b_d}} \\ \gamma_u(Q^2) &= \gamma_u \\ \gamma_d(Q^2) &= \gamma_d\end{aligned}$$

¹²Since \mathcal{D}_s already vanishes at $Q^2 = Q_0^2$, we have set it to zero in the whole small- Q^2 region.

6.3 Dataset and systematic errors

In the small- Q^2 region ($W^2 \geq 12.5 \text{ GeV}^2$, $Q^2 \leq 6.76 \text{ GeV}^2$), we shall fit the same quantities as previously and the data coming from the same collaborations:

- F_2^p : H1 [22, 23, 24, 27], ZEUS [30, 31, 32, 33, 34, 35], NMC [38], E665 [37], SLAC [39],
- F_2^d : BCDMS, NMC [38], E665 [37], SLAC [45],
- F_2^n/F_2^p : NMC [41],
- $F_2^{\nu N}$ and $xF_3^{\nu N}$: CCFR [44].

Concerning the treatment of the systematic errors, we have used the same correction factors as the ones obtained in the DGLAP global fit for the papers containing data in both the small- and the large- Q^2 region and leave this factor free for the papers containing only data at small Q^2 .

6.4 Results

The parametrisations described above have been fitted to the 948 data in the small- Q^2 region using MINUIT. The results of this fit, experiments by experiments, together with the parameter values is presented in Tables 3 and 4. We see that, apart from the ZEUS 1995 data and the CCFR F_2 data, we obtain a good description of the structure functions in the low- Q^2 region. The χ^2 per data point is quite good, considering that we have applied Regge theory to quite a large region as compared to usual approaches [13, 46, 47, 15, 48, 49]. The poor description of the ZEUS 1995 data may come from the fact that the systematic uncertainties have been fixed in the DGLAP fit.

The results for the structure functions in the low- Q^2 region are shown in Figures 3 to 15 together with the large- Q^2 results. In the small- Q^2 region, the curves are only drawn in the fitted region ($W^2 > 12.5 \text{ GeV}^2$). We see that the experimental measurements are well reproduced.

Finally, the curves in Figure 2 show the parton distribution functions obtained at small Q^2 . It is interesting to notice that valence quarks are large at small Q^2 and $W^2 \approx 12.5 \text{ GeV}^2$ which, in this case, correspond to small values of x . For example at $Q^2 = 0.1 \text{ GeV}^2$ and $x = 0.008$, we have $x\bar{u} \approx 0.043$, $x\bar{d} \approx 0.053$, $xu_V \approx 0.057$ and $xd_V \approx 0.019$.

7 DGLAP vs. Regge at high Q^2

7.1 Motivation

As we have shown in [17], we can consider that Regge theory also applies at large Q^2 . In these conditions, since Q^2 -dependent singularities are forbidden in Regge

theory, we expect a triple-pole behaviour at all values of Q^2 . The unphysical essential singularity generated by DGLAP evolution should therefore be considered as a numerical approximation to a triple-pole pomeron at small x .

Given these considerations, we have shown [17] that, using both forward and backward evolution, it is possible to describe the small- x experimental data with parton distribution functions of the form

$$A(Q^2) \log^2(1/x) + B(Q^2) \log(1/x) + C(Q^2) + D(Q^2)x^\eta$$

where the Q^2 -dependent couplings are extracted from the DGLAP evolution equation.

7.2 Parametrisation and uncertainties

In this QCD global fit, we would like to test if it is still possible to consider the result of the evolution as an approximation to a triple-pole. To achieve this task, we shall fit the parton distribution functions at each value of Q^2 with the following form

$$\begin{aligned} xu_V &= \frac{2}{N_u^*} x^\eta (1 + \gamma_u x) (1 - x)^{b_u}, \\ xd_V &= \frac{1}{N_d^*} x^\eta (1 + \gamma_d x) (1 - x)^{b_d}, \\ xu_s &= [A \log^2(1/x) + B \log(1/x) + C + D_u x^\eta] (1 - x)^b, \\ xd_s &= [A \log^2(1/x) + B \log(1/x) + C + D_d x^\eta] (1 - x)^b, \\ xs_s &= N_s [A \log^2(1/x) + B \log(1/x) + C + D_s x^\eta] (1 - x)^b, \\ xc_s &= N_c [A \log^2(1/x) + B \log(1/x) + C + D_c x^\eta] (1 - x)^b, \\ xb_s &= N_b [A \log^2(1/x) + B \log(1/x) + C + D_b x^\eta] (1 - x)^b, \\ xg &= [A_g \log^2(1/x) + B_g \log(1/x) + C_g^*] (1 - x)^{b+1}, \end{aligned}$$

Before performing this fit, we shall determine an uncertainty on the parton distribution. Since we want to show that the DGLAP evolution generates an essential singularity which mimics a triple-pole behaviour, we should estimate the error introduced by the evolution. Since we have used LO DGLAP evolution, we estimate that the errors are of the order of the NLO corrections:

$$q_{\text{NLO}}(x, Q^2) \approx (1 \pm \alpha_s(Q^2)) q_{\text{LO}}(x, Q^2).$$

If we require that the intimal parton distribution at $Q^2 = Q_0^2$ remains fixed, this leads to

$$q_{\text{NLO}}^{\text{norm}}(x, Q^2) \approx \frac{1 \pm \alpha_s(Q^2)}{1 \pm \alpha_s(Q_0^2)} q_{\text{LO}}(x, Q^2),$$

or, keeping only the leading term in the strong coupling constant,

$$\Delta q(x, Q^2) = |\alpha_s(Q_0^2) - \alpha_s(Q^2)| q_{\text{LO}}(x, Q^2).$$

In addition, we shall take into account the fact that, at small Q^2 , there may also be higher-twist corrections. If we assume¹³ these are at 5% at $Q^2 = Q_0^2$, we shall finally consider

$$\Delta q(x, Q^2) = \left[|\alpha_s(Q_0^2) - \alpha_s(Q^2)| + \frac{0.05 Q_0^2}{(1-x)Q^2} \right] q_{LO}(x, Q^2).$$

Finally, additional powers of $1-x$ are expected to describe the large- x behaviour of the parton distributions at large Q^2 , hence we shall only consider the region $10^{-5} \leq x \leq 0.1$ for the sea quarks and the gluons. For the case of the valence quarks, we hope that the factor $(1+\gamma x)$ is sufficient to reproduce the distribution for $10^{-5} \leq x \leq 1$.

7.3 Results

To perform the fit, we have taken the parton distributions with their estimated uncertainties in 80 points regularly spaced in $\log(x)$. Since the parametrisations for the valence quarks and the sea quarks have disjoint parameters, we have performed two different fits at each Q^2 . The result of these are presented at Figure 8 for $Q^2 = 100 \text{ GeV}^2$ and $Q^2 = 10000 \text{ GeV}^2$. In addition, the predictions for the triple-pole residues for F_2^p are shown at figure 8 together with the χ^2 per point of the fit.

We clearly see that the parametrisation works very well for valence quarks at all values of Q^2 , as well as for the u_s and d_s distributions. For heavy quarks and gluons, although the χ^2/nop remains less than 1, there are some discrepancies between the DGLAP essential singularity and the triple-pole fit at small x and large Q^2 . However, these differences are only present for $\sqrt{s} > 3 \text{ TeV}$, which means that it is impossible to distinguish between the two approaches in present experimental measurements. This high-energy region should be reached at the LHC and should provide very useful information to distinguish between the different models.

Moreover, we have also tried to estimate the uncertainties on the parton densities in another way. We have considered the uncertainties obtained from the DGLAP fit at $Q^2 = Q_0^2$:

$$q(x, Q_0^2) - \Delta q(x, Q_0^2) \leq q(x, Q_0^2) \leq q(x, Q_0^2) + \Delta q(x, Q_0^2).$$

We can then evolve $q(x, Q_0^2) \pm \Delta q(x, Q_0^2)$ and using these quantities to obtain the uncertainties at all values of Q^2 . If we do so, we obtain very similar conclusions.

8 Conclusions and perspectives

We have seen that we can use Regge theory to constrain the initial parton densities at $Q^2 = Q_0^2$ and obtain the distributions at higher virtualities with the DGLAP

¹³This value reproduces errors comparable with those obtained from our uncertainties estimation. In addition, the higher-twist term is relevant for middle-range values of Q^2 while the subleading corrections are important at large Q^2 .

evolution equation. In this approach, Regge theory is used to describe the low- Q^2 data and QCD applies at large Q^2 . In such a way, the complex- j -plane singularities are common to parton distribution functions in the initial condition and to soft amplitudes which provides a unified description at high-energy in the soft region.

We have also shown in this paper that it is possible to *define* the parton distributions in the low- Q^2 region and to parametrise them using Regge theory. This parametrisation is useful to describe the DIS structure functions but should be used with care. Actually, since factorisation is not proven at small Q^2 , we cannot ensure that the parton distributions can be extended to $Q^2 = 0$. Using our parametrisation to describe processes such as jet production may be incorrect.

Considering the low- Q^2 parametrisation together with the Global QCD fit, we have a combined description of the hadronic structure functions over the whole Q^2 range. This model, consistent with DGLAP evolution and with Regge theory, reproduces the experimental measurements with a very good χ^2 .

In addition, we extended the approach of [16] to $x = 1$ using only forward evolution. We have not applied the techniques developed in [17] and extracted the Q^2 behaviour of the fitted parameters by combining forward and backward evolution. The reason is that, even with a few parameters, there often exist multiple minima and it is quite hard to obtain a continuous result for all parameters. This situation is expected to be even worse with the parametrisation used here due to the larger number of parameters. Hence, in order to test the compatibility between the DGLAP-evolved parton distributions and a triple-pole parametrisation, we have shown that the parton densities can be approximated by a $\log^2(1/x)$ behaviour at small x and large Q^2 . This approximation works very well up to $\sqrt{s} \approx 3$ TeV, and at which point it deviates from DGLAP for the heavy quarks and the gluons. This means that we expect high-energy corrections to be important in this domain and that the LHC should provide very useful information to distinguish between the different high-energy models. In this high-energy region, one should expect contributions from the BFKL equation as well as unitarity and saturation effects.

Finally, a NLO analysis will be performed in the near future. This gives a much more reliable description of the data, allows a more complete comparison with other parametrisations and gives a description of the F_c and F_L structure functions.

Acknowledgements

First of all, I would like to thank J.R. Cudell for very useful discussions and suggestions. I am also very grateful to L. Favart and J. Stirling. Finally, I would like to thank Y.K. Yang for fruitful discussions concerning the CCFR measurements. This work is supported by the National Fund for Scientific Research (FNRS), Belgium.

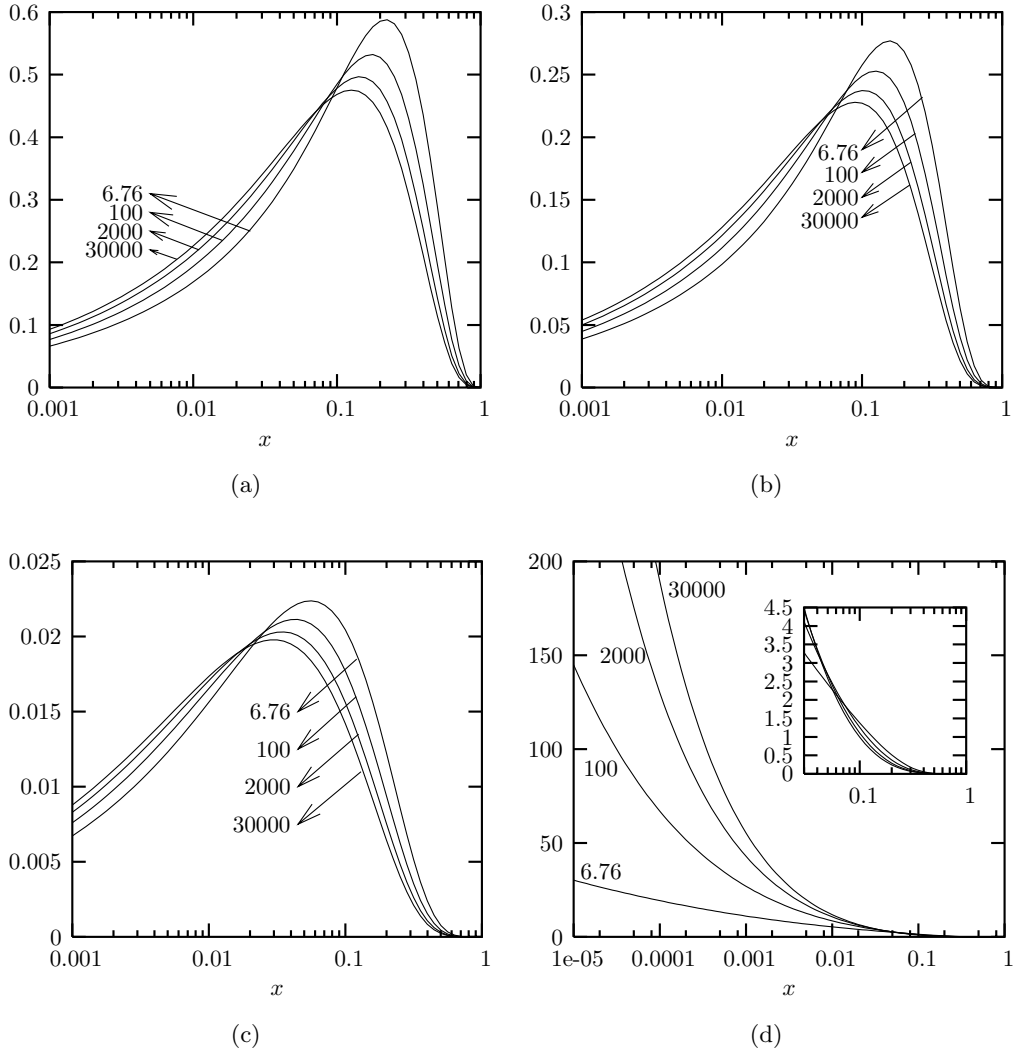


Figure 1: Typical momentum distributions inside the proton at various Q^2 : (a) u valence quarks, (b) d valence quarks, (c) sea asymmetry $\bar{d} - \bar{u}$ and (d) gluon distribution.

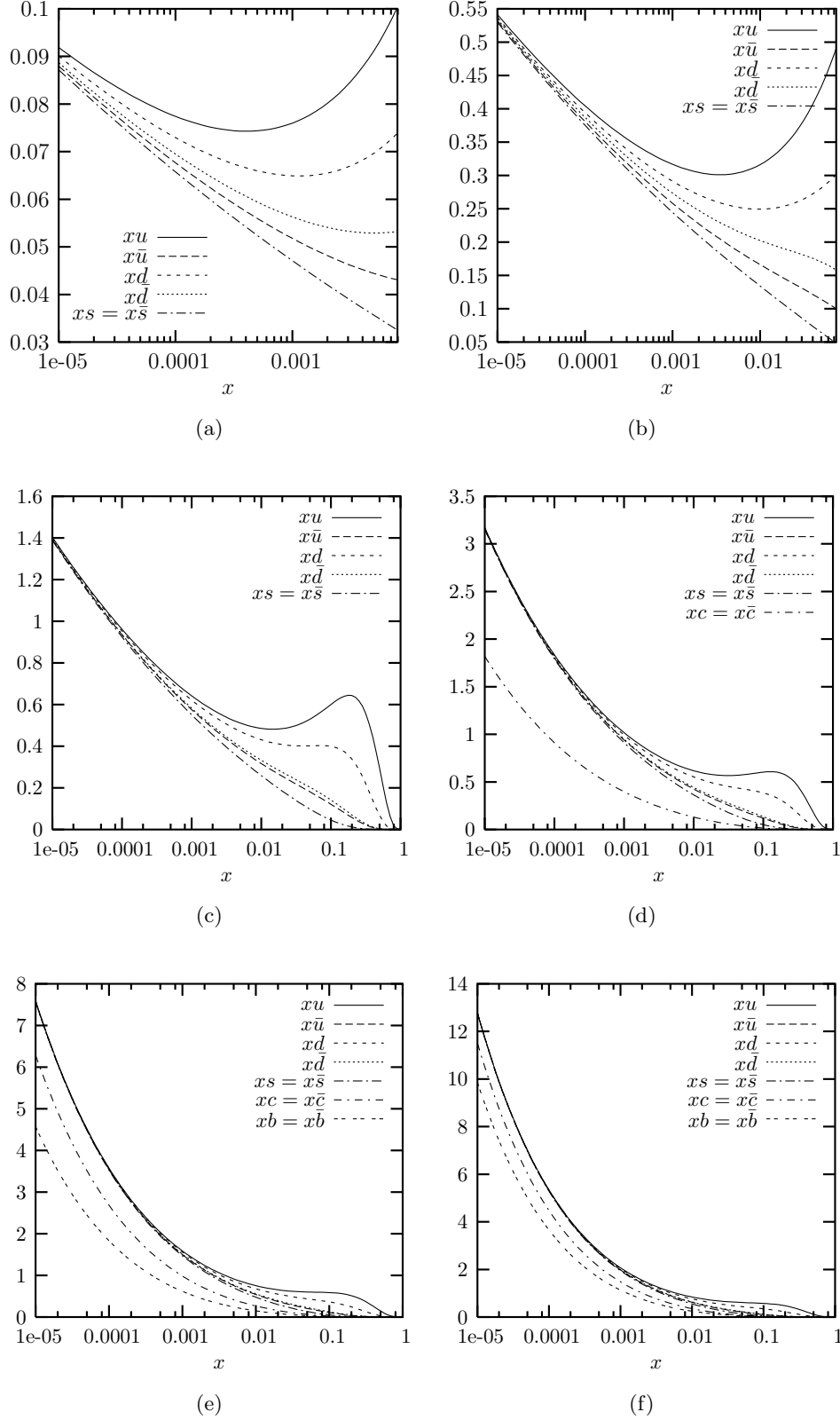


Figure 2: Quark distributions inside the proton at various Q^2 : (a) $Q^2 = 0.1 \text{ GeV}^2$, (b) $Q^2 = 1 \text{ GeV}^2$, (c) $Q^2 = Q_0^2 = 4m_c^2$, (d) $Q^2 = 4m_b^2$, (e) $Q^2 = 2000 \text{ GeV}^2$ and (f) $Q^2 = 30000 \text{ GeV}^2$. See 6.2 for details concerning the parton distributions at

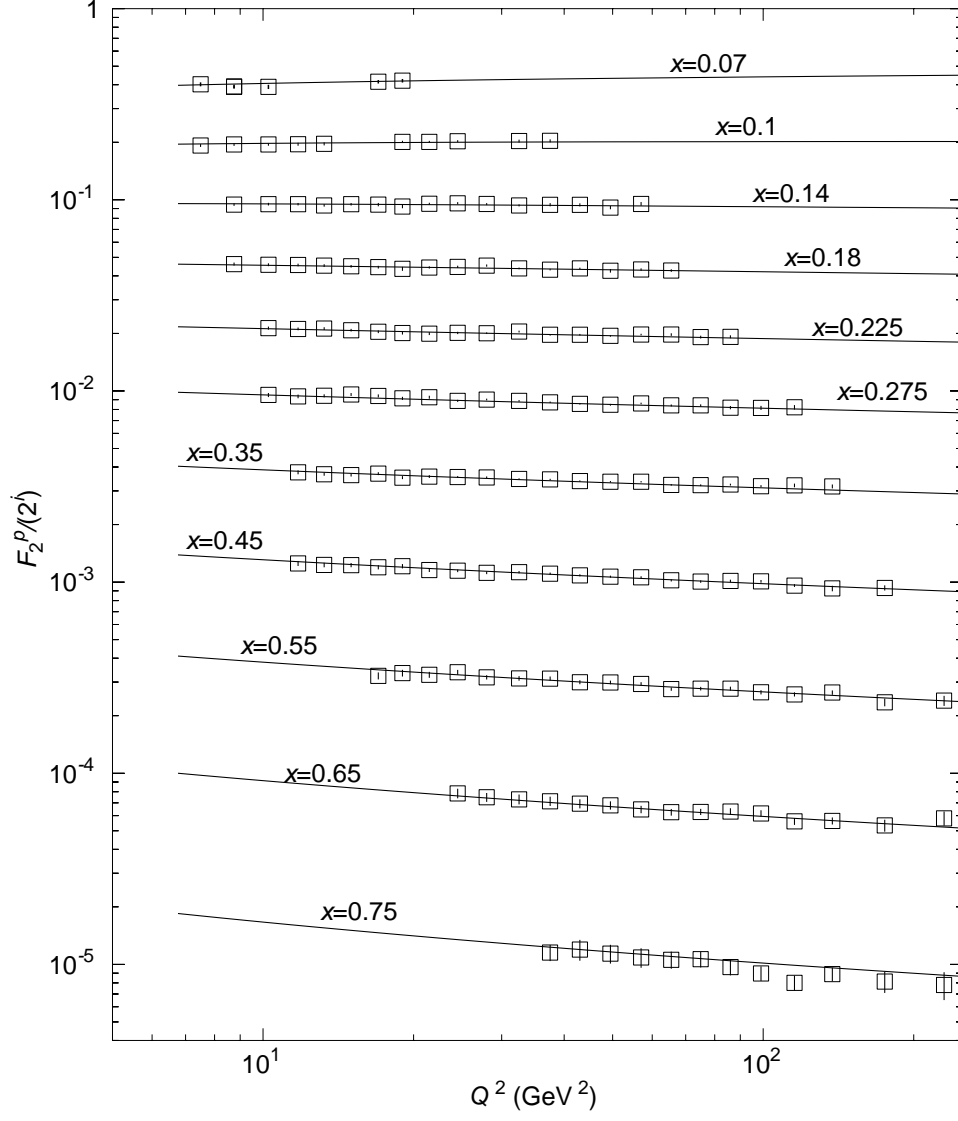


Figure 3: DGLAP evolution results for BCDMS F_2^p data ($i = 0$ for the upper curve and is increased by 1 from one curve to the next one).

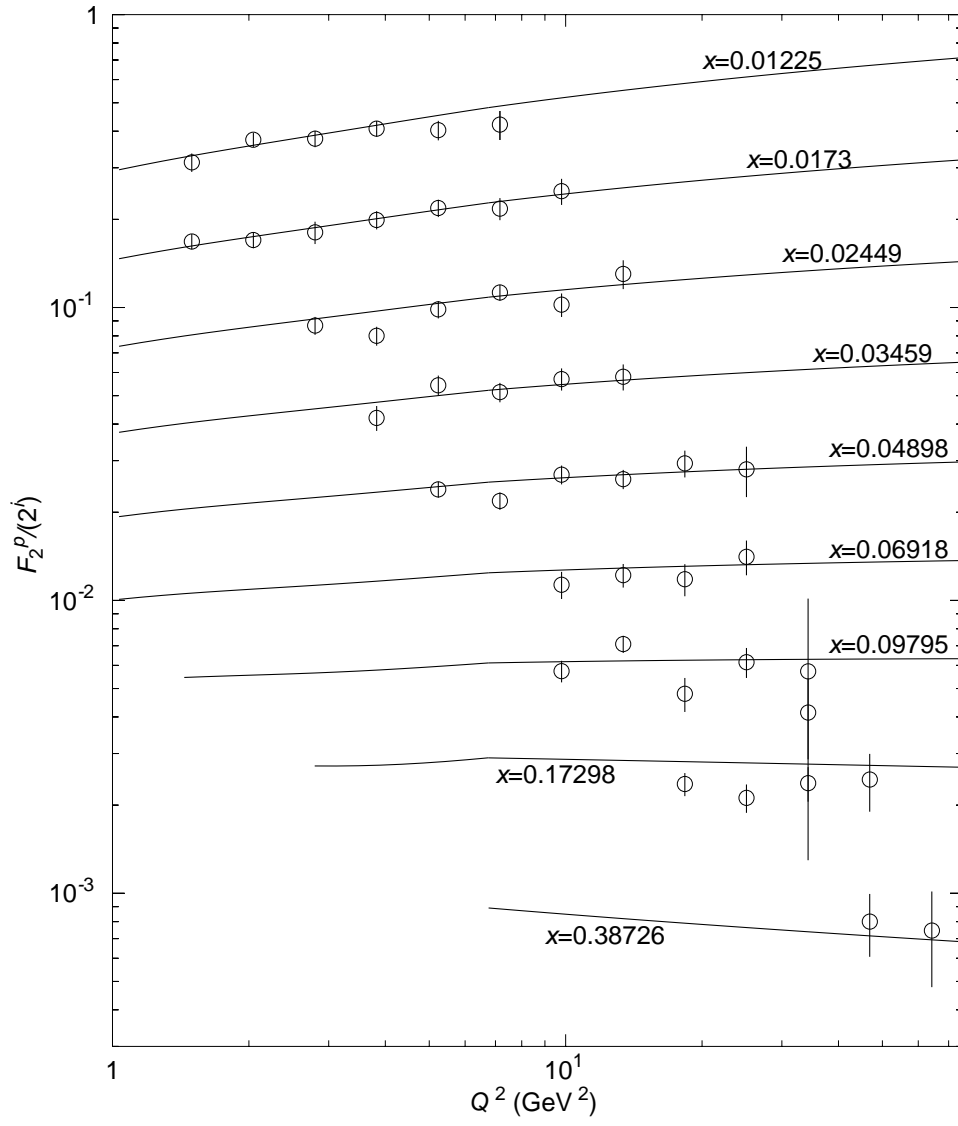


Figure 4: DGLAP evolution results for E665 F_2^p data. $i = 0$ for the upper curve and is increased by 1 from one curve to the next one.

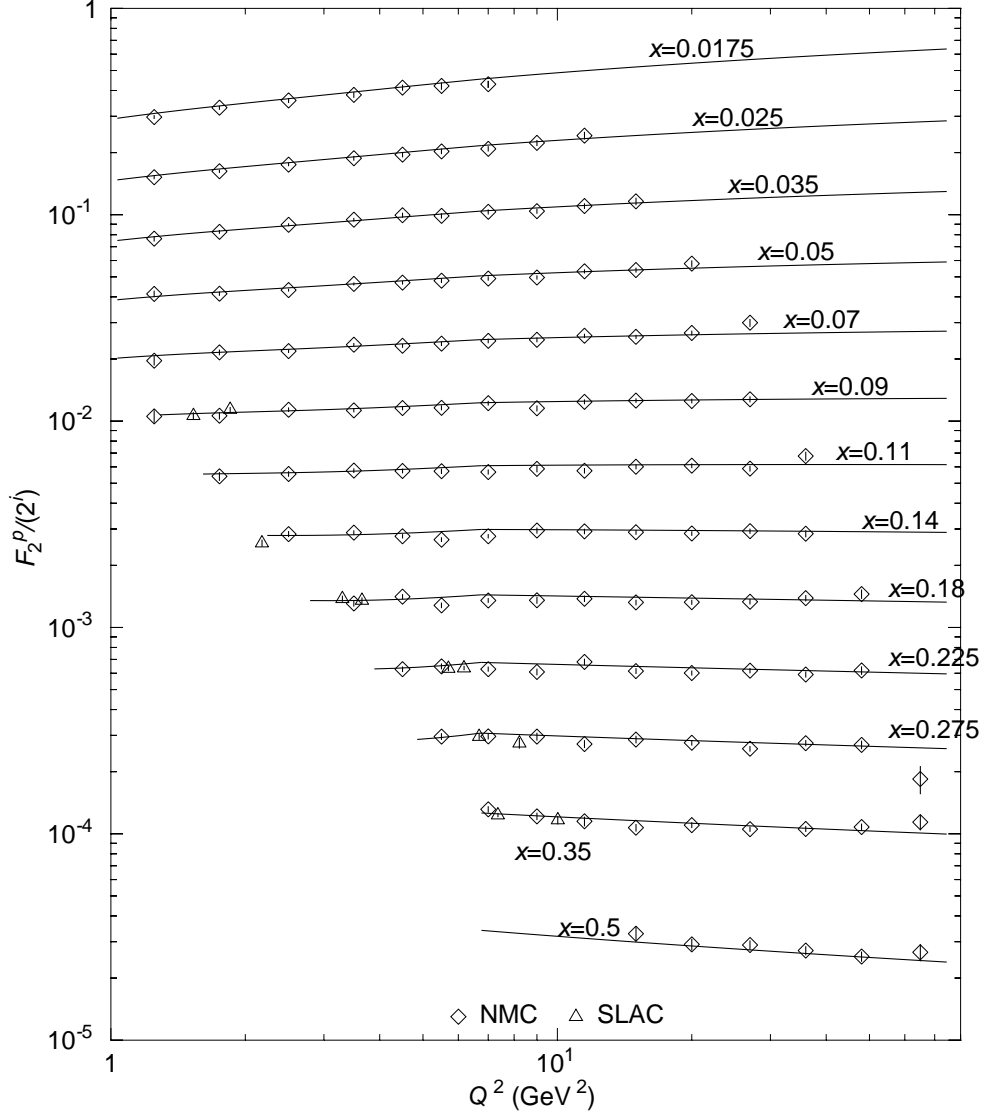


Figure 5: DGLAP evolution results for NMC F_2^p data (the SLAC data appearing in the NMC Q^2 bins have been added to the plot). $i = 0$ for the upper curve and is increased by 1 from one curve to the next one.

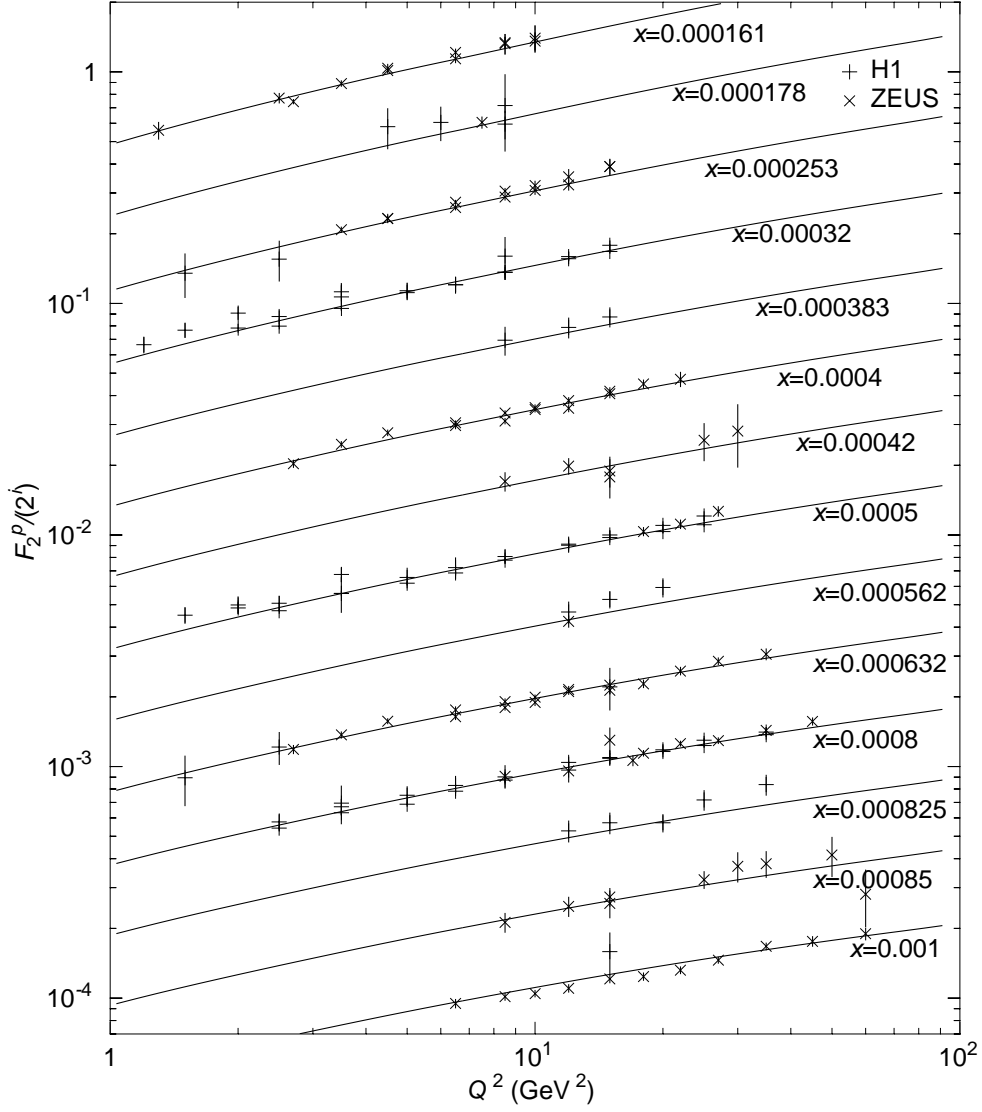


Figure 6: DGLAP evolution results for HERA F_2^p data ($x \leq 0.001$). $i = 0$ for the upper curve and is increased by 1 from one curve to the next one.

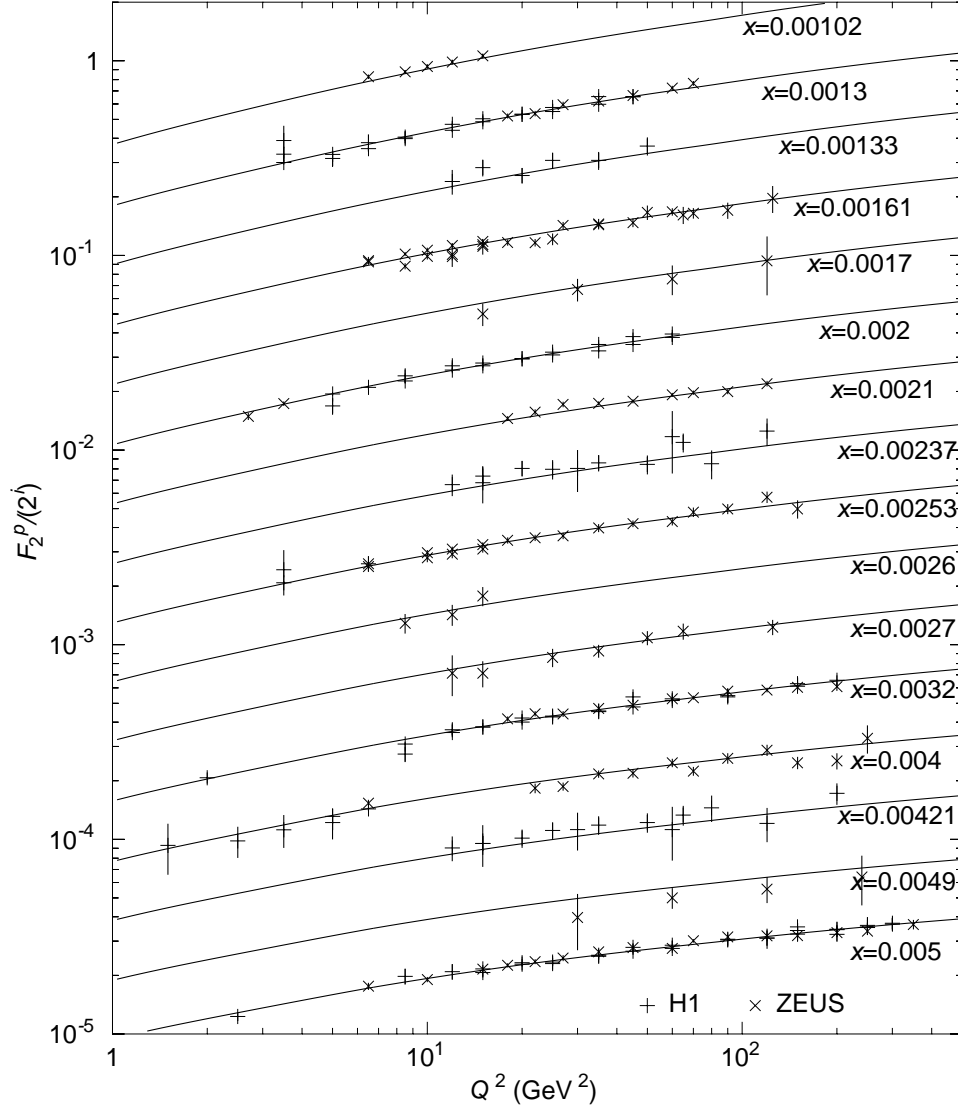


Figure 7: DGLAP evolution results for HERA F_2^p data ($0.001 < x \leq 0.005$). $i = 0$ for the upper curve and is increased by 1 from one curve to the next one.

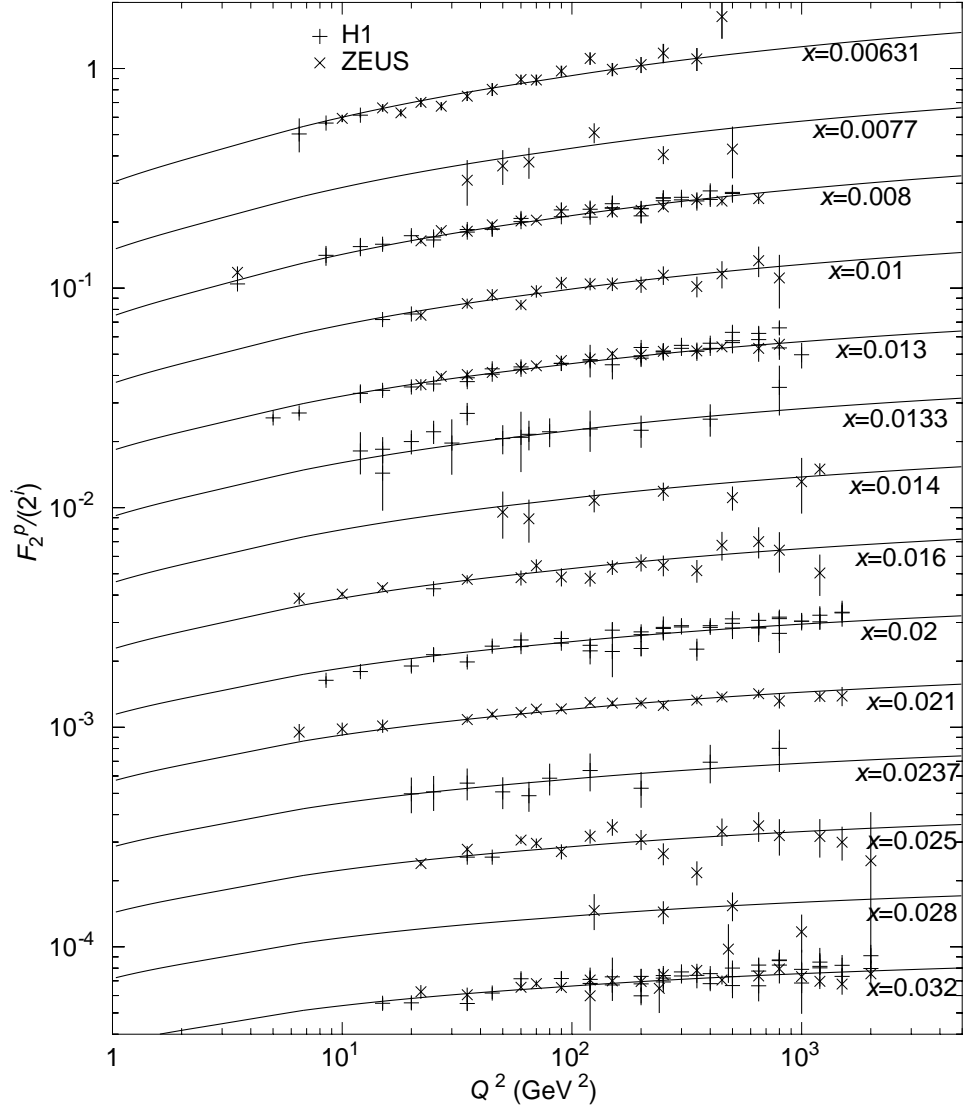


Figure 8: DGLAP evolution results for HERA F_2^p data ($0.005 < x \leq 0.04$). $i = 0$ for the upper curve and is increased by 1 from one curve to the next one.

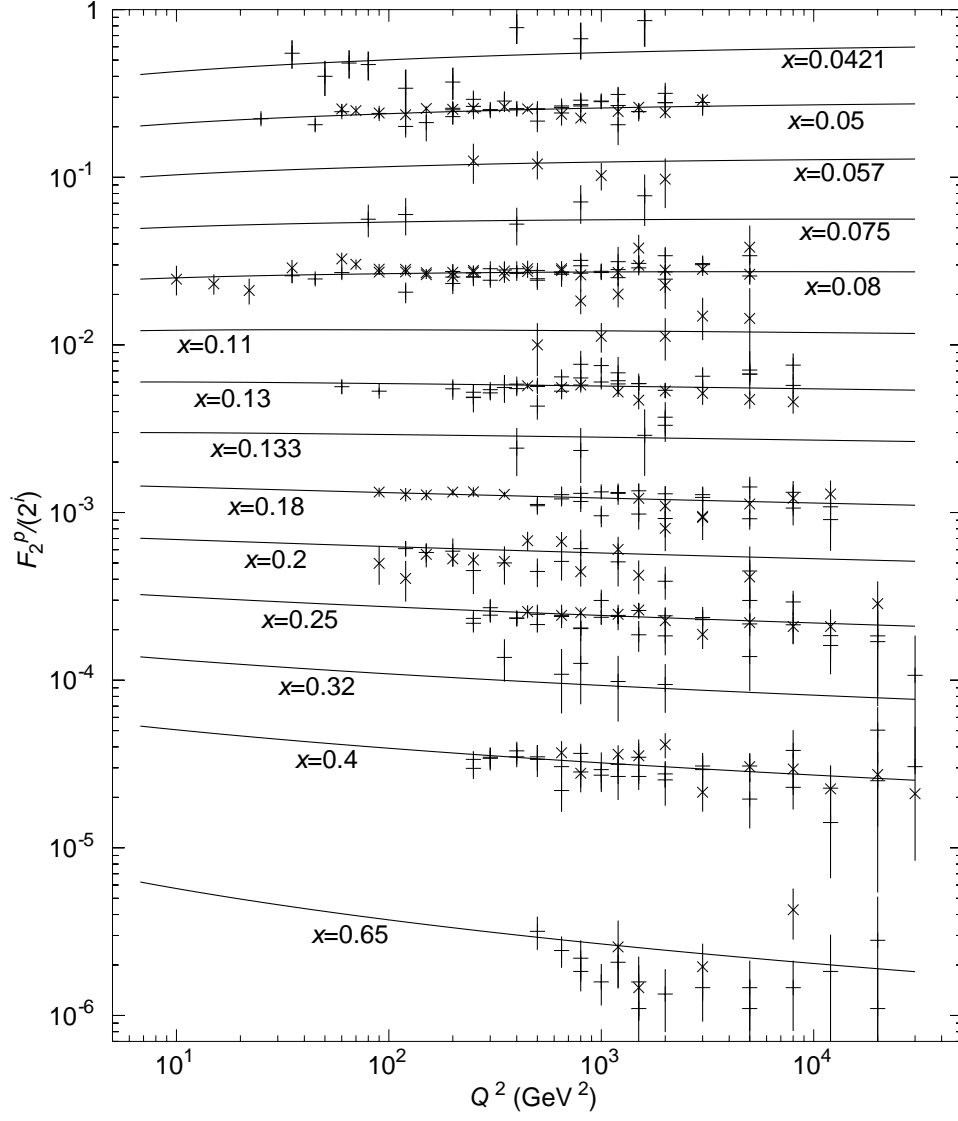


Figure 9: DGLAP evolution results for HERA F_2^p data ($0.04 < x$). $i = 0$ for the upper curve and is increased by 1 from one curve to the next one.

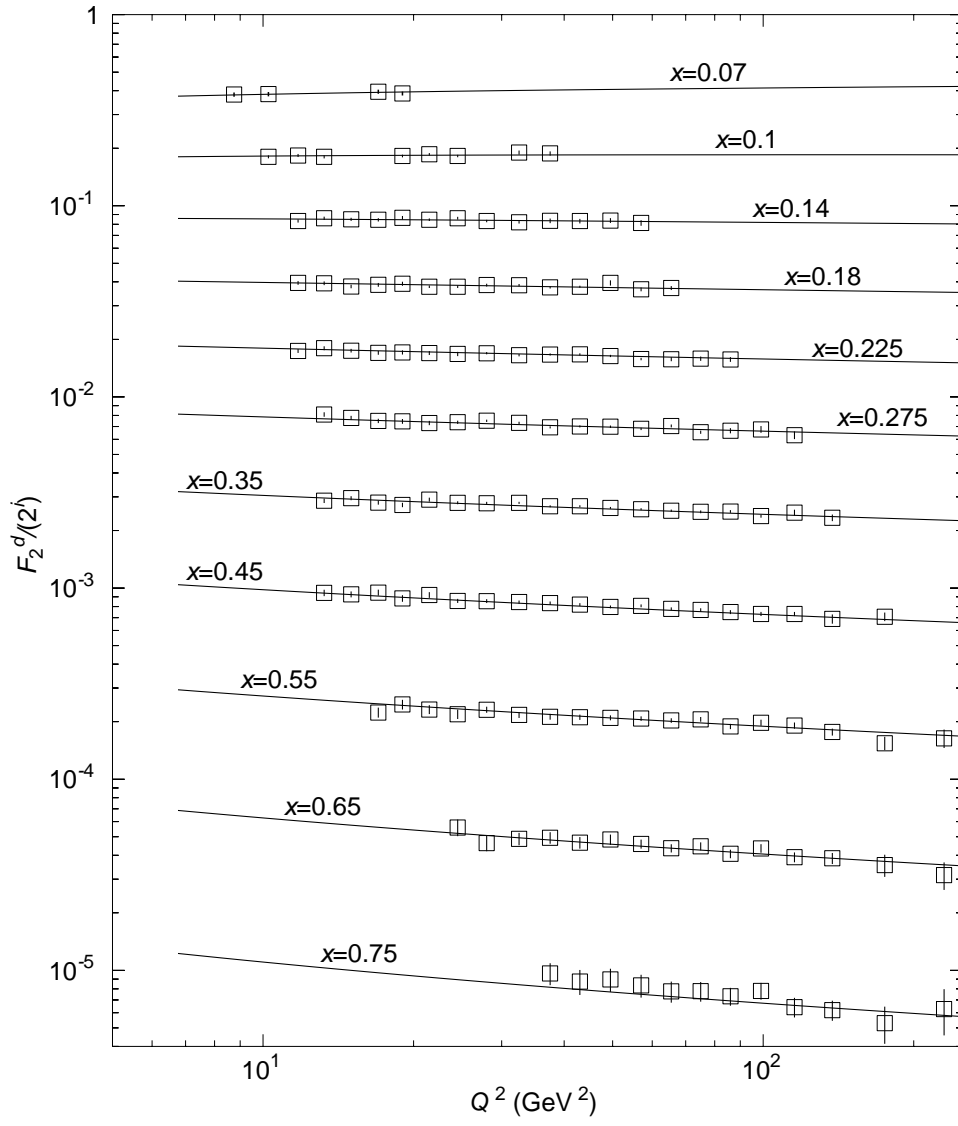


Figure 10: DGLAP evolution results for BCDMS F_2^d data. $i = 0$ for the upper curve and is increased by 1 from one curve to the next one.

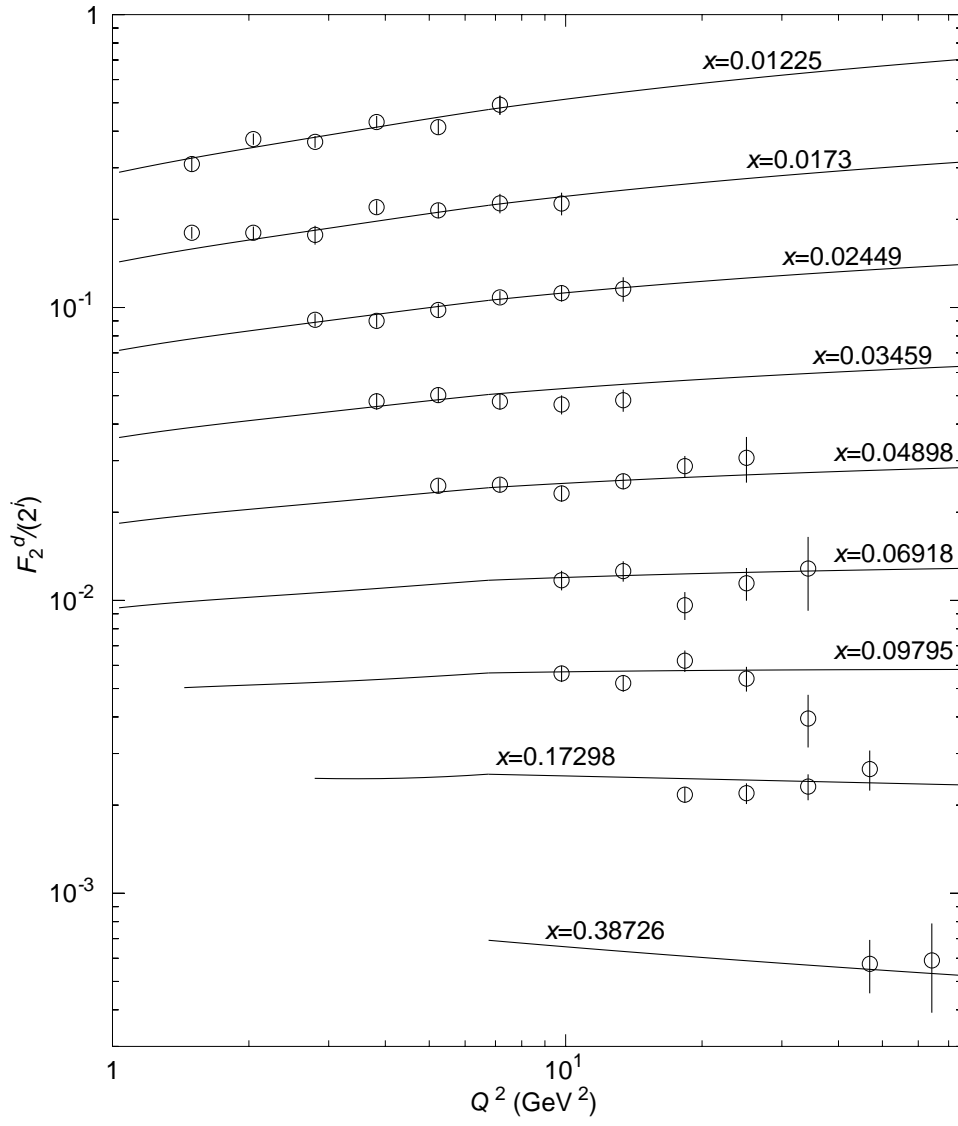


Figure 11: DGLAP evolution results for E665 F_2^d data. $i = 0$ for the upper curve and is increased by 1 from one curve to the next one.

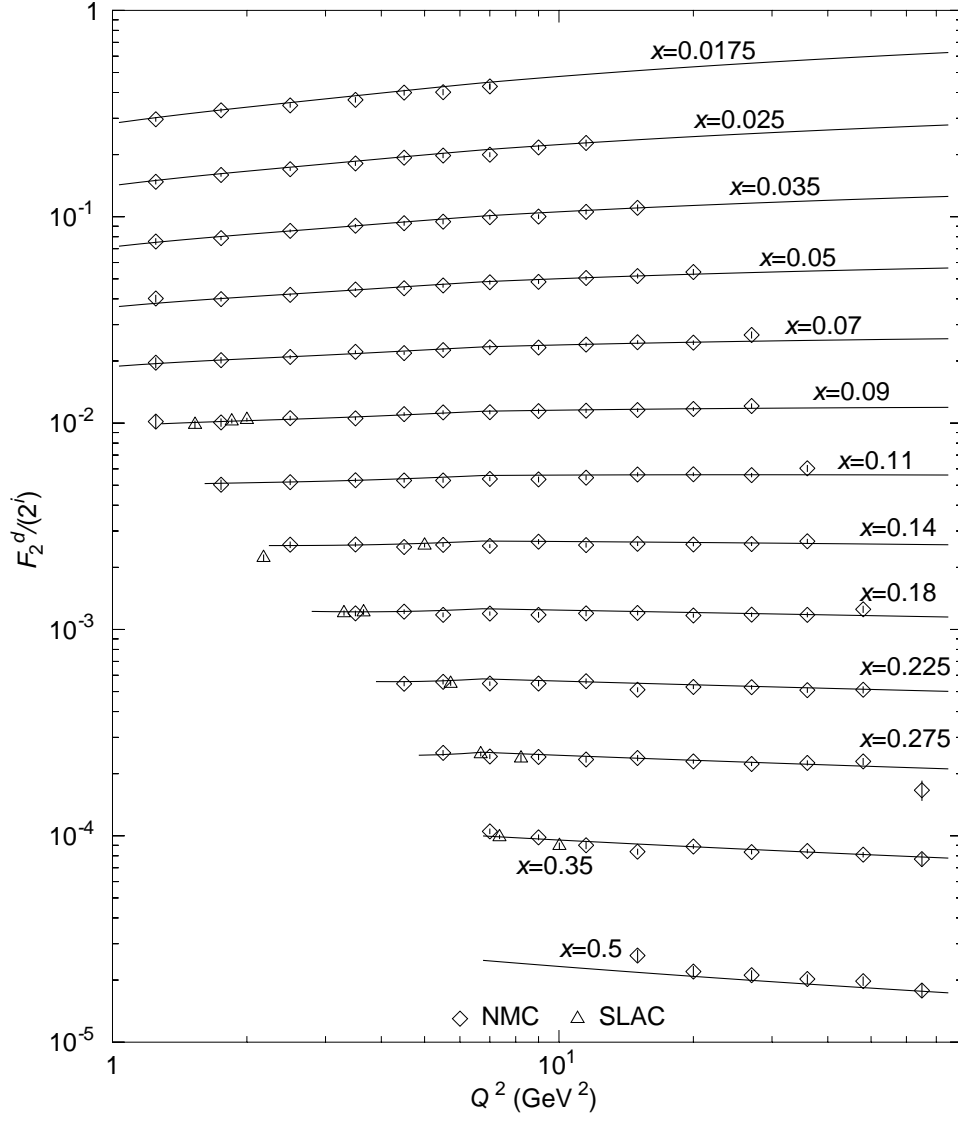


Figure 12: DGLAP evolution results for NMC F_2^d data (the SLAC data appearing in the NMC Q^2 bins have been added to the plot). $i = 0$ for the upper curve and is increased by 1 from one curve to the next one.

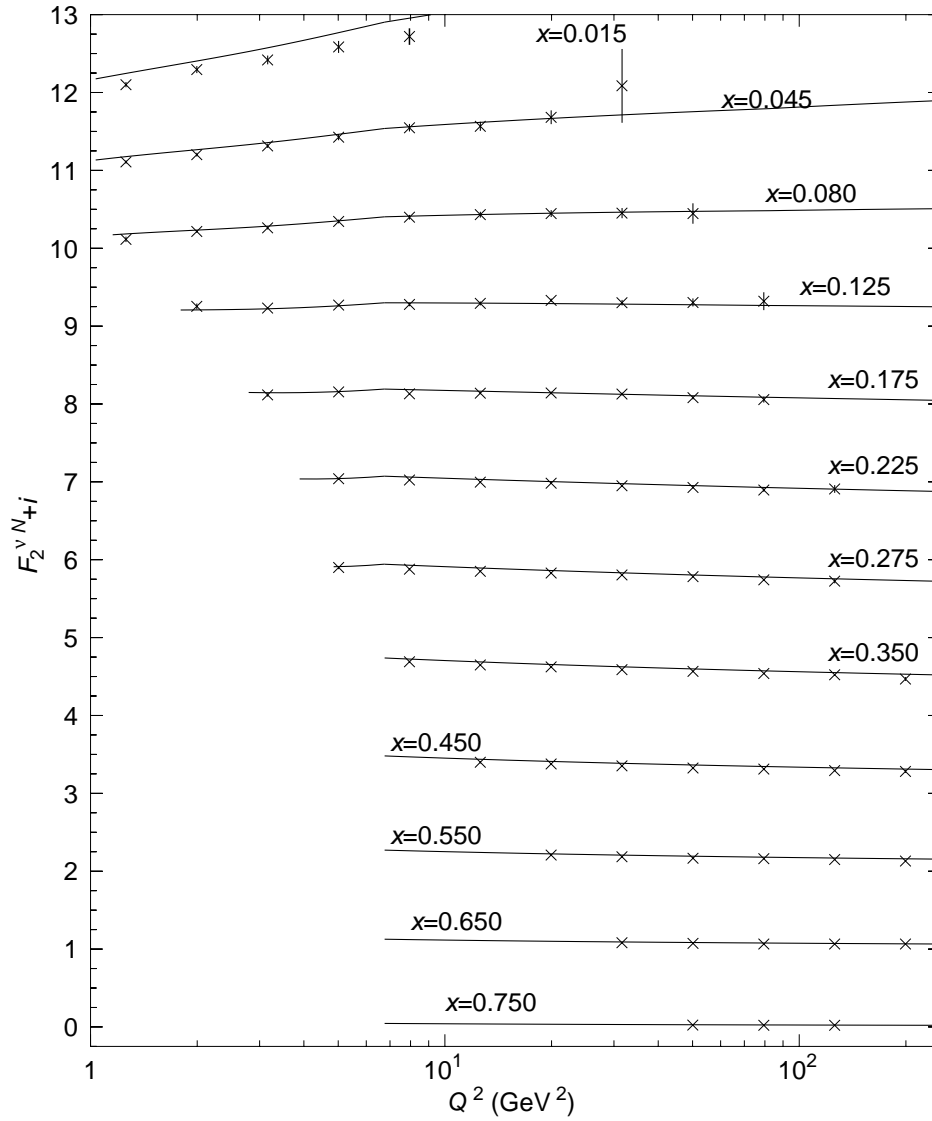


Figure 13: DGLAP evolution results for CCFR $F_2^{\nu N}$ data. $i = 0$ for the upper curve and is increased by 1 from one curve to the next one.

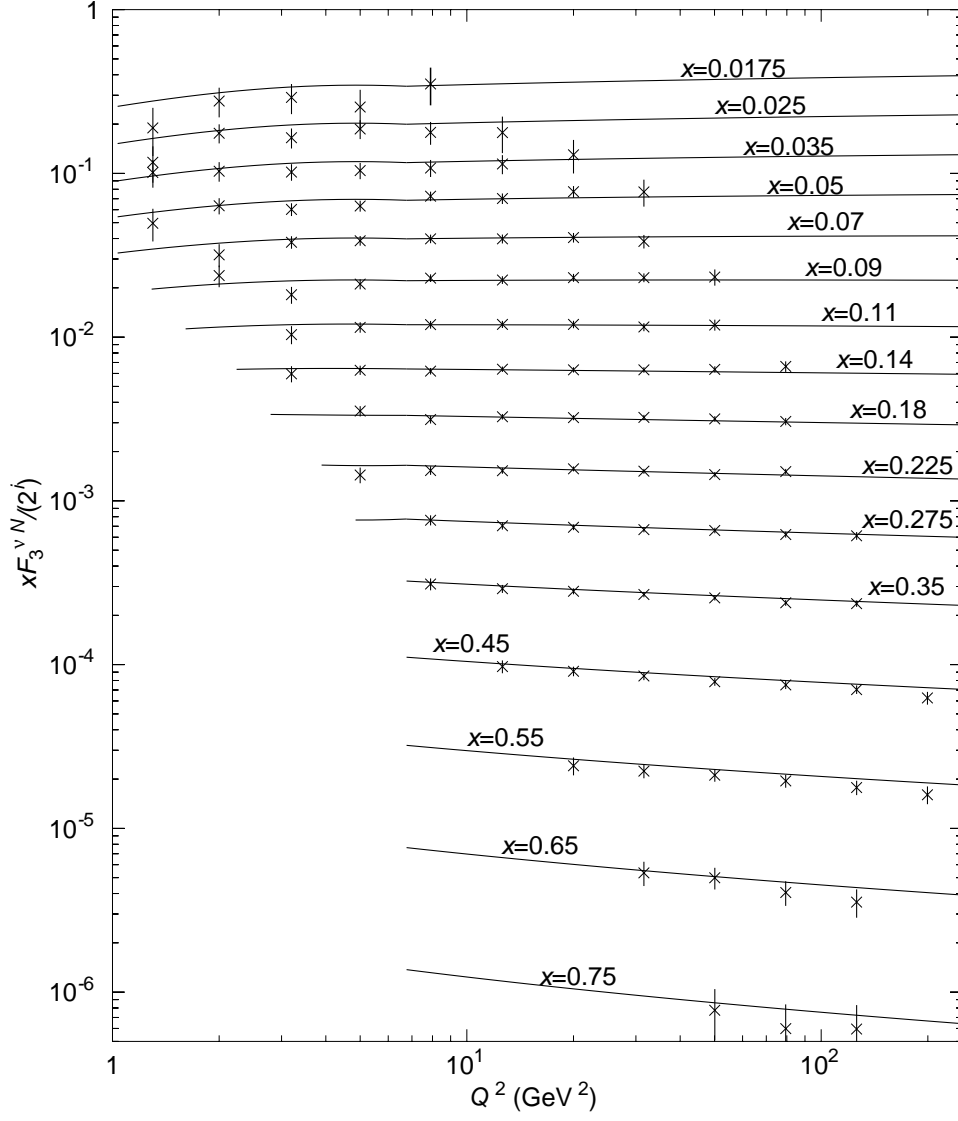


Figure 14: DGLAP evolution results for CCFR $xF_3^{\nu N}$ data. $i = 0$ for the upper curve and is increased by 1 from one curve to the next one.

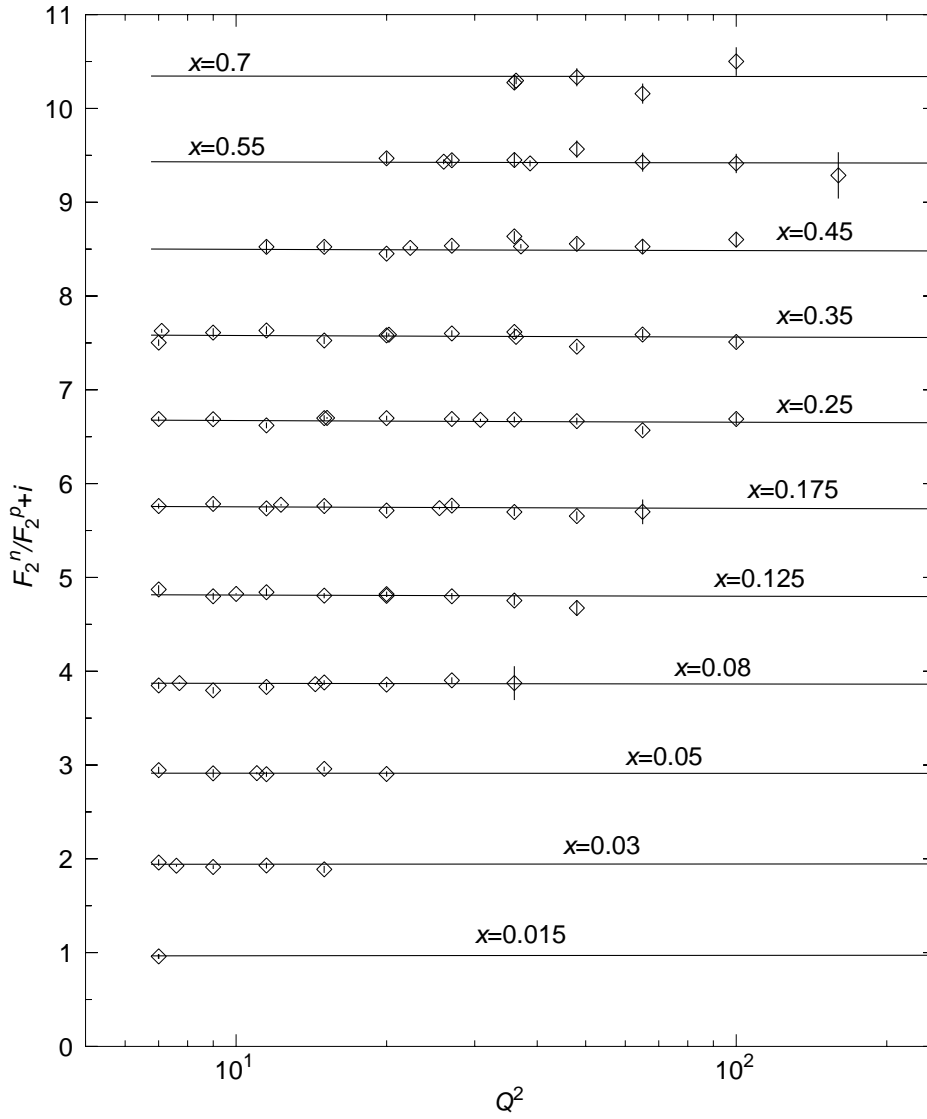


Figure 15: DGLAP evolution results for NMC F_2^n/F_2^p data. $i = 0$ for the upper curve and is increased by 1 from one curve to the next one.

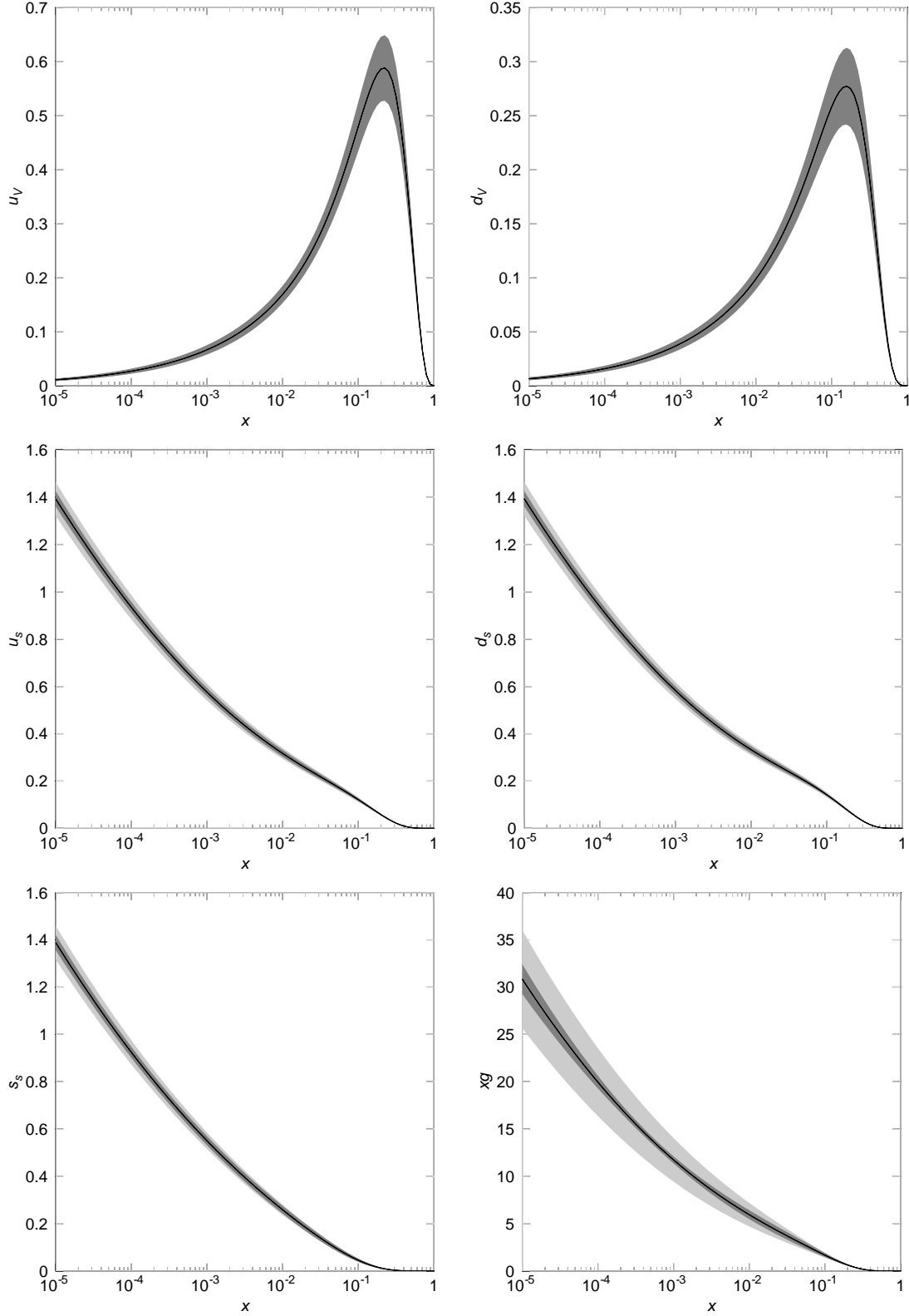


Figure 16: Initial distributions with their uncertainties: the dark region represents the correlated uncertainties while the light one is obtained without taking into account the correlations between the parameters.

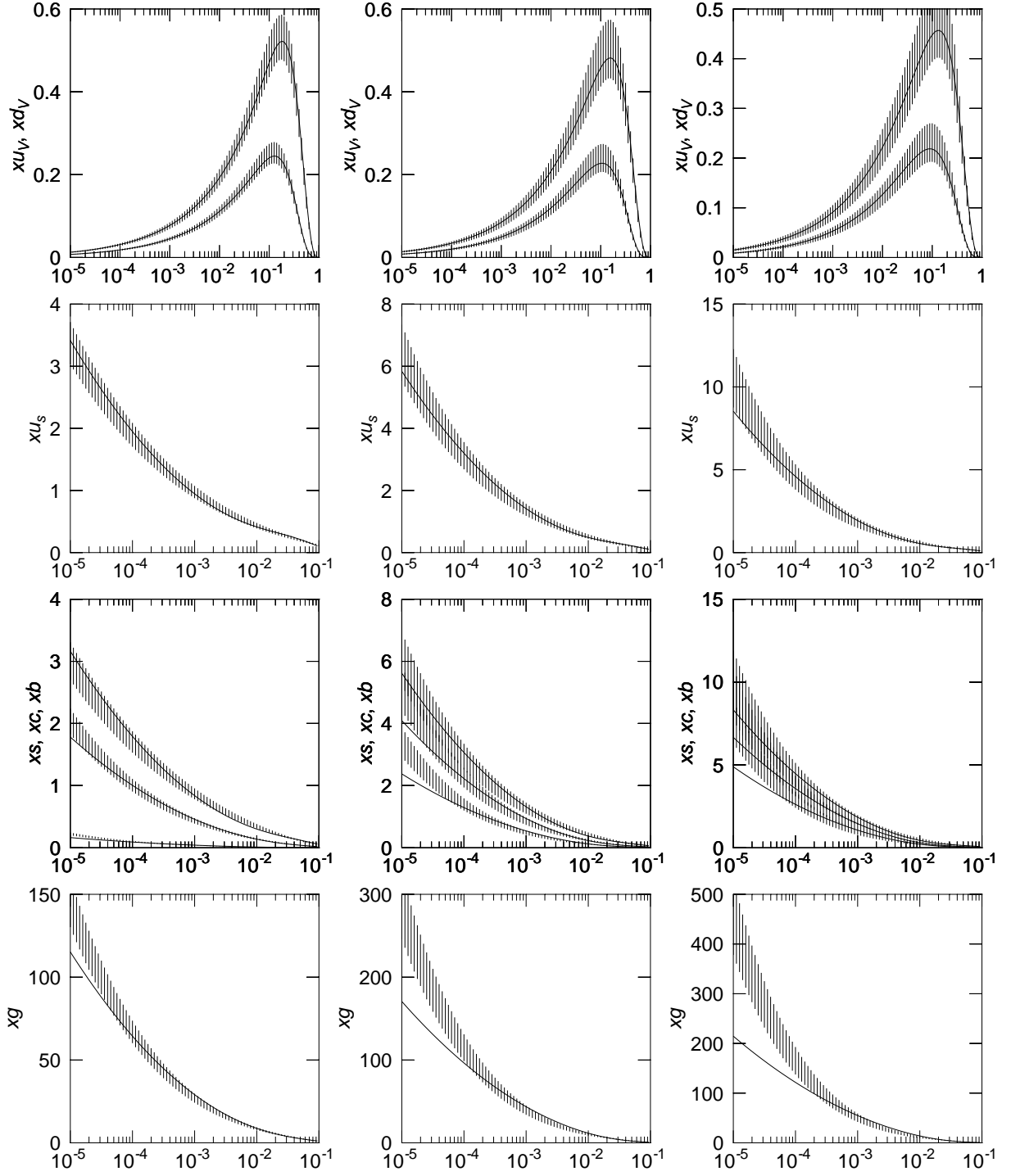


Figure 17: Triple-pole pomeron fit to the parton distribution functions obtained from DGLAP evolution. The first column shows distributions at $Q^2 = 100 \text{ GeV}^2$, the second corresponds to $Q^2 = 1000 \text{ GeV}^2$ and the third to $Q^2 = 10000 \text{ GeV}^2$.

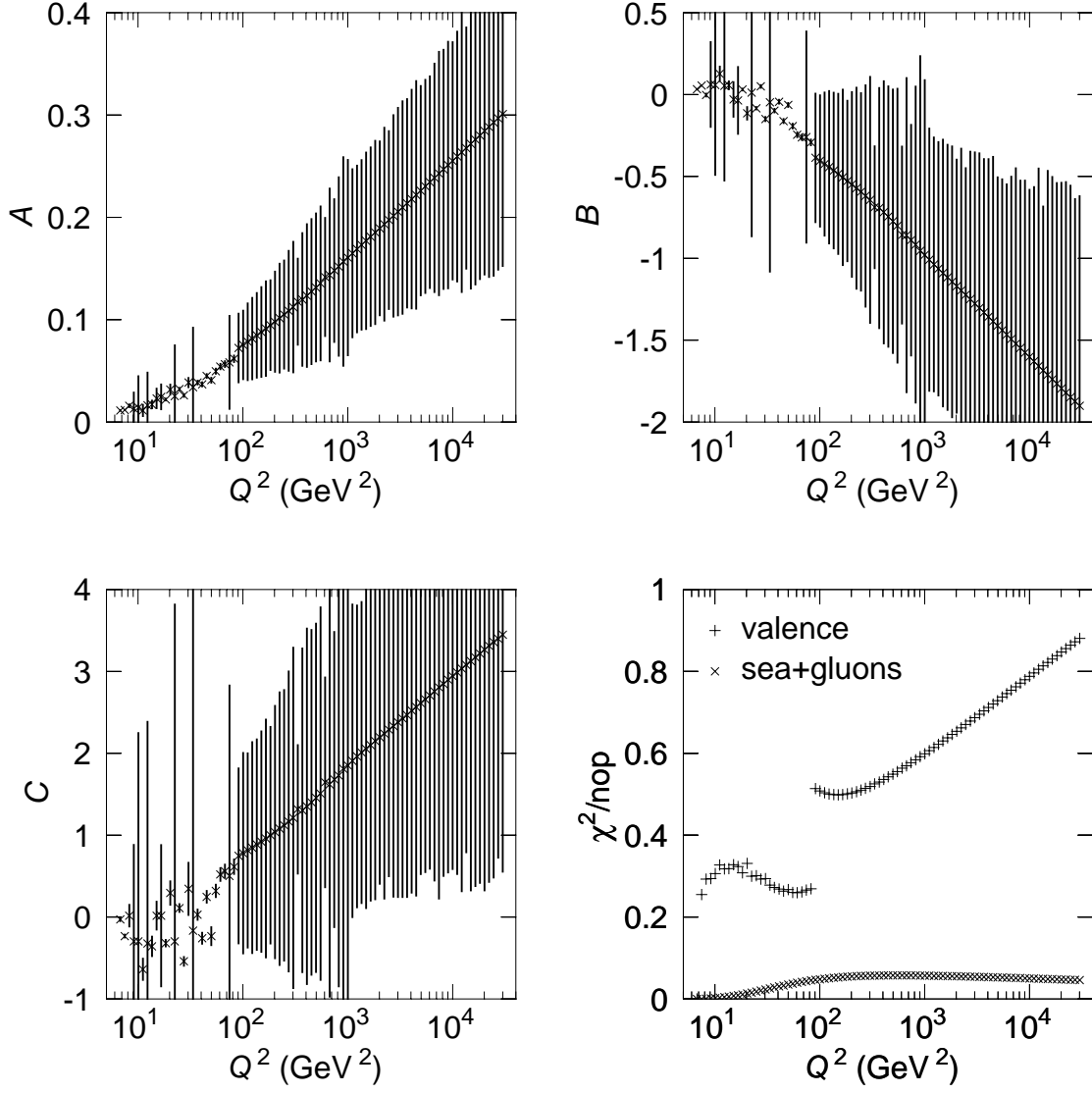


Figure 18: Triple-pole form factors for F_2^p at large Q^2 presented together with the result of the fit of a triple pole to the large- Q^2 parton densities/.

Param.	global	A	B	C	D_u	D_d	D_s	A_g	B_g	γ_u	γ_d	b_u	b_d	b	η
A	0.99650	1.000	-0.895	-0.015	0.733	0.631	0.007	-0.363	0.268	0.365	0.304	0.018	-0.022	0.442	-0.368
B	0.99824	-0.895	1.000	0.025	-0.864	-0.668	-0.006	0.229	-0.148	-0.567	-0.494	-0.081	-0.042	-0.589	0.562
C	0.28980	-0.015	0.025	1.000	0.005	0.005	0.000	0.001	-0.002	0.001	0.001	0.001	0.000	0.000	0.002
D_u	0.99222	0.733	-0.864	0.005	1.000	0.822	0.006	0.086	-0.177	0.524	0.521	0.267	0.085	0.876	-0.460
D_d	0.98233	0.631	-0.668	0.005	0.822	1.000	0.005	-0.071	-0.009	0.110	0.040	0.397	-0.243	0.762	-0.009
D_s	0.02647	0.007	-0.006	0.000	0.006	0.005	1.000	0.001	-0.002	0.005	0.005	0.004	0.000	0.008	-0.004
A_g	0.99616	-0.363	0.229	0.001	0.086	-0.071	0.001	1.000	-0.980	0.346	0.380	0.253	0.199	0.356	-0.291
B_g	0.99649	0.268	-0.148	-0.002	-0.177	-0.009	-0.002	-0.980	1.000	-0.403	-0.443	-0.317	-0.228	-0.464	0.332
γ_u	0.99956	0.365	-0.567	0.001	0.524	0.110	0.005	0.346	-0.403	1.000	0.900	0.253	0.318	0.518	-0.980
γ_d	0.99665	0.304	-0.494	0.001	0.521	0.040	0.005	0.380	-0.443	0.900	1.000	0.081	0.648	0.552	-0.893
b_u	0.97469	0.018	-0.081	0.000	0.267	0.397	0.004	0.253	-0.317	0.253	0.081	1.000	-0.232	0.537	-0.073
b_d	0.97329	-0.022	-0.042	0.000	0.085	-0.243	0.000	0.199	-0.228	0.318	0.648	-0.232	1.000	0.174	-0.332
b	0.99685	0.442	-0.589	0.002	0.876	0.762	0.008	0.356	-0.464	0.518	0.552	0.537	0.174	1.000	-0.389
η	0.99965	-0.368	0.562	-0.001	-0.460	-0.009	-0.004	-0.291	0.332	-0.980	-0.893	-0.073	-0.332	-0.389	1.000

Table 5: Fitted parameters correlation coefficients.

A Momentum sum rule and gluon distribution

In this appendix, we shall give the expression of the constant in the gluon distribution, constrained by the momentum sum rule. Recall that we have, at $Q^2 = Q_0^2$,

$$\begin{aligned}
xu_V(x) &= \frac{2}{N_u} x^\eta (1 + \gamma_u x) (1 - x)^{b_u}, \\
xd_V(x) &= \frac{1}{N_d} x^\eta (1 + \gamma_d x) (1 - x)^{b_d}, \\
x\bar{q}_i(x) &= [A \log^2(1/x) + B \log(1/x) + C + D_i x^\eta] (1 - x)^b, \\
xg(x) &= [A_g \log^2(1/x) + B_g \log(1/x) + C_g] (1 - x)^{b+1},
\end{aligned} \tag{5}$$

where N_q is given by equation (2). We shall use momentum conservation to constrain the constant term C_g in the gluon distribution. Let us first introduce the special functions that we need. The Euler Gamma function is defined by

$$\Gamma(x) = \int_0^\infty dt t^{x-1} e^{-t}.$$

We can then introduce the Beta function $B(x, y)$, the digamma function $\Psi(x)$ and the polygamma function $\Psi^{(m)}(x)$ related to the gamma functions by the following formulæ

$$\begin{aligned}
B(x, y) &= \frac{\Gamma(x)\Gamma(y)}{\Gamma(x+y)}, \\
\Psi(x) &= \frac{\partial_x \Gamma(x)}{\Gamma(x)}, \\
\Psi^{(m)}(x) &= \partial_x^m \Psi(x).
\end{aligned}$$

With these definitions, the momenta carried by the distributions (5) are given by the following expressions:

$$\begin{aligned}
p_{u_V} &= \frac{2\eta}{b_u + \eta + 1} \left(1 + \gamma_u \frac{\eta + 1}{b_u + \eta + 2} \right) \left(1 + \gamma_u \frac{\eta}{b_u + \eta + 1} \right)^{-1}, \\
p_{d_V} &= \frac{\eta}{b_d + \eta + 1} \left(1 + \gamma_d \frac{\eta + 1}{b_d + \eta + 2} \right) \left(1 + \gamma_d \frac{\eta}{b_d + \eta + 1} \right)^{-1}, \\
p_{\bar{q}_i} &= \frac{1}{b+1} \left(A \left\{ [\gamma_E + \Psi(b+2)]^2 - \Psi^{(1)}(b+2) + \frac{\pi^2}{6} \right\} + B [\gamma_E + \Psi(b+2)] + C \right) \\
&\quad + D_i B(b+1, \eta+1), \\
p_g &= \frac{1}{b_g + 1} \left(A_g \left\{ [\gamma_E + \Psi(b_g+2)]^2 - \Psi^{(1)}(b_g+2) + \frac{\pi^2}{6} \right\} + B_g [\gamma_E + \Psi(b_g+2)] + C_g \right).
\end{aligned}$$

From the proton, momentum conservation gives

$$p_g + p_{u_V} + p_{d_V} + 2(p_{\bar{u}} + p_{\bar{d}} + p_{\bar{s}}) = 1,$$

and we finally obtain

$$c_G = A_g \left\{ [\gamma_E + \Psi(b_g + 2)]^2 - \Psi^{(1)}(b_g + 2) + \frac{\pi^2}{6} \right\} + B_g [\gamma_E + \Psi(b_g + 2)] \\ + (b_g + 1) [1 - p_{u_V} - dp_V - 2(p_{\bar{u}} + p_{\bar{d}} + p_{\bar{s}})].$$

References

- [1] V.N. Gribov and L.N. Lipatov, *Sov. J. Nucl. Phys.* **15** (1972) 438; G. Altarelli and G. Parisi, *Nucl. Phys.* **B126** (1977) 298; Yu.L. Dokshitzer, *Sov. Phys. JETP* **46** (1977) 641.
- [2] A. D. Martin, R. G. Roberts, W. J. Stirling and R. S. Thorne, *Eur. Phys. J. C* **23**, 73 (2002) [arXiv:hep-ph/0110215].
- [3] M. Gluck, E. Reya and A. Vogt, *Eur. Phys. J. C* **5**, 461 (1998) [arXiv:hep-ph/9806404].
- [4] J. Pumplin, D. R. Stump, J. Huston, H. L. Lai, P. Nadolsky and W. K. Tung, *JHEP* **0207**, 012 (2002) [arXiv:hep-ph/0201195].
- [5] A. M. Cooper-Sarkar, *J. Phys. G* **28**, 2669 (2002) [arXiv:hep-ph/0205153].
- [6] S. I. Alekhin, *Phys. Rev. D* **63**, 094022 (2001) [arXiv:hep-ph/0011002].
- [7] V. S. Fadin, E. A. Kuraev and L. N. Lipatov, *Phys. Lett. B* **60** (1975) 50. L. N. Lipatov, *Sov. J. Nucl. Phys.* **23** (1976) 338 [*Yad. Fiz.* **23** (1976) 642]. I. I. Balitsky and L. N. Lipatov, *Sov. J. Nucl. Phys.* **28** (1978) 822 [*Yad. Fiz.* **28** (1978) 1597].
- [8] V. S. Fadin and L. N. Lipatov, *JETP Lett.* **49** (1989) 352 [*Yad. Fiz.* **50** (1989) SJNCA,50,712.1989) 1141].
- [9] The reader who wants a modern overview of S -matrix and Regge theory and diffraction can read the books S. Donnachie, G. Dosch, P. Landshoff and O. Nachtmann, *Pomeron Physics and QCD* (Cambridge University Press, Cambridge, 2002), and V. Barone and E. Predazzi, *High-Energy Particle Diffraction* (Springer, Berlin Heidelberg, 2002).
- [10] T. Regge, *Nuovo Cim.* **14** (1959) 951.
- [11] T. Regge, *Nuovo Cim.* **18** (1960) 947.
- [12] K. Hagiwara et al., *Review of Particle Physics*, *Phys. Rev. D* **66** (2002) 010001. The data on total cross-sections can be obtained from <http://pdg.lbl.gov>.
- [13] A. Donnachie and P. V. Landshoff, *Phys. Lett. B* **518** (2001) 63 [arXiv:hep-ph/0105088].

- [14] J. R. Cudell and G. Soyez, Phys. Lett. B **516** (2001) 77 [arXiv:hep-ph/0106307].
- [15] P. Desgrolard and E. Martynov, Eur. Phys. J. C **22** (2001) 479 [arXiv:hep-ph/0105277].
- [16] G. Soyez, arXiv:hep-ph/0211361.
- [17] G. Soyez, arXiv:hep-ph/0306113.
- [18] A. Donnachie and P. V. Landshoff, Phys. Lett. B **533** (2002) 277 [arXiv:hep-ph/0111427].
- [19] L. Csernai, L. Jenkovszky, K. Kontros, A. Lengyel, V. Magas and F. Paccanoni, Eur. Phys. J. C **24** (2002) 205 [arXiv:hep-ph/0112265].
- [20] C. Lopez and F. J. Yndurain, Nucl. Phys. B **171** (1980) 231.
- [21] I. Abt *et al.* [H1 Collaboration], Nucl. Phys. B **407** (1993) 515.
- [22] T. Ahmed *et al.* [H1 Collaboration], Nucl. Phys. B **439** (1995) 471 [arXiv:hep-ex/9503001].
- [23] S. Aid *et al.* [H1 Collaboration], Nucl. Phys. B **470** (1996) 3 [arXiv:hep-ex/9603004].
- [24] C. Adloff *et al.* [H1 Collaboration], Nucl. Phys. B **497** (1997) 3 [arXiv:hep-ex/9703012].
- [25] C. Adloff *et al.* [H1 Collaboration], Eur. Phys. J. C **13** (2000) 609 [arXiv:hep-ex/9908059].
- [26] C. Adloff *et al.* [H1 Collaboration], Eur. Phys. J. C **19** (2001) 269 [arXiv:hep-ex/0012052].
- [27] C. Adloff *et al.* [H1 Collaboration], Eur. Phys. J. C **21** (2001) 33 [arXiv:hep-ex/0012053].
- [28] M. Derrick *et al.* [ZEUS Collaboration], Phys. Lett. B **316** (1993) 412.
- [29] M. Derrick *et al.* [ZEUS Collaboration], Z. Phys. C **65** (1995) 379.
- [30] M. Derrick *et al.* [ZEUS Collaboration], Z. Phys. C **69** (1996) 607 [arXiv:hep-ex/9510009].
- [31] M. Derrick *et al.* [ZEUS Collaboration], Z. Phys. C **72** (1996) 399 [arXiv:hep-ex/9607002].
- [32] J. Breitweg *et al.* [ZEUS Collaboration], Phys. Lett. B **407** (1997) 432 [arXiv:hep-ex/9707025].

- [33] J. Breitweg *et al.* [ZEUS Collaboration], Eur. Phys. J. C **7** (1999) 609 [arXiv:hep-ex/9809005].
- [34] J. Breitweg *et al.* [ZEUS Collaboration], Eur. Phys. J. C **12** (2000) 35 [arXiv:hep-ex/9908012].
- [35] S. Chekanov *et al.* [ZEUS Collaboration], Eur. Phys. J. C **21** (2001) 443 [arXiv:hep-ex/0105090].
- [36] A. C. Benvenuti *et al.* [BCDMS Collaboration], Phys. Lett. B **223** (1989) 485.
- [37] M. R. Adams *et al.* [E665 Collaboration], Phys. Rev. D **54** (1996) 3006.
- [38] M. Arneodo *et al.* [New Muon Collaboration], Nucl. Phys. B **483** (1997) 3 [arXiv:hep-ph/9610231].
- [39] L. W. Whitlow, E. M. Riordan, S. Dasu, S. Rock and A. Bodek, Phys. Lett. B **282** (1992) 475.
- [40] A. C. Benvenuti *et al.* [BCDMS Collaboration], Phys. Lett. B **237** (1990) 595.
- [41] P. Amaudruz *et al.* [New Muon Collaboration], Nucl. Phys. B **371** (1992) 3.
- [42] E. Oltman *et al.*, Z. Phys. C **53** (1992) 51.
- [43] W. G. Seligman *et al.*, Phys. Rev. Lett. **79** (1997) 1213.
- [44] B. T. Fleming *et al.* [CCFR Collaboration], Phys. Rev. Lett. **86** (2001) 5430 [arXiv:hep-ex/0011094].
- [45] S. Dasu *et al.*, Phys. Rev. D **49** (1994) 5641.
- [46] L. L. Jenkovszky, F. Paccanoni and E. Predazzi, Nucl. Phys. Proc. Suppl. **25B** (1992) 80.
- [47] P. Desgrolard, M. Giffon, L. L. Enkovsky, A. I. Lengyel and E. Predazzi, Phys. Lett. B **309** (1993) 191.
- [48] J. R. Cudell, E. Martynov and G. Soyez, arXiv:hep-ph/0207196.
- [49] G. Soyez, arXiv:hep-ph/0401177.